UNIVERSIDADE NOVA DE LISBOA

FACULDADE DE CIÊNCIAS E TECNOLOGIA

DEPARTAMENTO DE QUÍMICA

David Miguel Baião Barata

"Production of recombinant protein hLIF in static and dynamic systems of animal cell culture"

Thesis for the Degree of
Master of Science in Biotechnology
Universidade Nova de Lisboa,
Faculdade de Ciências e Tecnologia

Supervisor:
Professor Luís Fonseca
Instituto Superior Técnico (IST)
Universidade Técnica de Lisboa (UTL)

Co-Supervisor:
Doutor Ricardo Baptista (IST-UTL)

MONTE DE CAPARICA, 2009

Acknowledgements

This work was developed in the Stem Cell and Bioengineering Laboratory at BioEngineering Research Group (BERG) in Instituto Superior Técnico, under the supervision of Professor Luís Fonseca and co-supervision of Professor Cláudia Lobato da Silva and Doctor Ricardo Baptista.

In the academic world:

To professors Luís Fonseca, Joaquim Cabral and Cláudia Lobato da Silva for receiving me at Instituto Superior Técnico, as well for their supervision.

To Dr. Ricardo Baptista for being available for knowledge transfer and brightness in his observations along my work.

To the Master in Biotechnology coordination, in the person of Professor Susana Barreiros, for being available for their students, helping our academic and scientific development.

To Professor Ana Aguiar Ricardo for the help in finding such a thesis subject matching with my personal interest.

To Serviços de Acção Social for the financial support, hosting and friendship.

To BERG/IBB-IST* colleagues, for giving me great friendship, a ride into the daily canteen journey and in the informal knowledge transfer that I value so much.

In the world of friends:

They are so much and I surely don't want to miss anyone. More than my professional construct, I believe that my personality is a treasure born from their action, care and friendship, being an important part of me along this time. A special hug to Daniel Siva, Daniel Carretas, Sabrina Semitela and Inês Gomes, and other friends from Residência Fraústo da Silva (only photos can remember the good times), to my friends from BCM, Sofia Santos, Rita Piteira and Gustavo Patrício (*promoted to*) for the nights of study and the gastronomic leisure. To the super scientist, Paulo Severino, *the man who don't sleep,* thank a lot. To all my Rotaract and Interact good friends (Ângelo Afonso, Inês Costa,, Bruno Rodrigues, Marta Roque, Hugo Cunha, Luís Rodrigues, Elizabeth Correia, Félix José da Silva, Nuno Semedo, Rodolfo Pereira, and all the

others that I don’t mention here ...), thanks for helping me in learning a lot about friendship, leadership, and happiness (you are a huge part of me). To my friends from Castelo Branco, specially to Nelson Ribeiro & Tig (Andreia Correia), Hervé Almeida, and Wilson Inácio, you are the beginning of everything.

In the family world:

You are whom I most hold in line this years, always busy will a thousand of stuff, it is good to receive the warm smile of my father Luís Barata, from my mother Eugénia Barata and from my brother Pedro Barata (aka PM), always supporting me and building an example of family with a modest basis and integral principles. Even with distance we could fortify our connection and our way of being trough love.

To my grandmother “avó São” for the unconditional support, being an example to follow, showing always how to care and educate with confidence in the future. To my grandmother “avó Piedade” for the lesson of hard work and to my uncles special thanks for the example of integrity, adaptability and courage.

Finally to the princess of my neighbourhood, Joana Romão, I thank you for giving me a place to feel safe and confident. I hope the future could smile to us and together we will build something positive.

*** BERG/IBB-IST** is the BioEngineering Research Group from the Institute of Biotechnology and BioEngineering at Instituto Superior Técnico (Universidade Técnica de Lisboa)

Abstract

The present work focuses the optimization of the production of human Leukemia Inhibitory Factor (hLIF) by human embryonic kidney 293 (HEK293) - EBNA1 cell line cultured as suspension aggregates in spinner flask. The effects of initial cell density and feeding-regime in cellular growth and productivity were evaluated.

A first phase occurs until the end of exponential growth in medium containing serum, being followed by puromycin selection of cells containing hLIF plasmid. A second phase, the production phase, is developed under serum-free conditions. Three initial cell densities (2×10^4 cells.mL^{-1}, 2×10^5 cells.mL^{-1} and 2×10^6 cells.mL^{-1}) were tested and the effect on maximum cell density and cell aggregate size distribution was evaluated. The inoculum of 2×10^5 cells.mL^{-1} led to final higher cellular densities around 7×10^6 cells.mL^{-1} and homogeneous aggregates around 278 μm were observed. The effect of the feeding-regime was then studied for the production of recombinant hLIF with an initial cell density of 2×10^5 cells.mL^{-1} by performing metabolite analysis

Metabolite analysis revealed the occurrence of glucose and glutamine starvation upon 9 and 7 days, respectively, in 25% FR. Therefore, glutamine acted as an alternative carbon, energy and aminoacid source in HEK293-EBNA1 growth. Observed lactate levels were bellow the inhibition limit concentrations (30 mM [1]). HEK293-EBNA1 did not seem to be affected by the produced levels of ammonia.

In conclusion, the 25% feeding regime at 2×10^5 cells.mL^{-1} initial cell density lead to the higher viable cell densities, either along culture time at growth and at production phase, with aggregates in suspension below necrotic diameters. This experiment conditions also allowed achieving the higher LIF volumetric productivity, 125 ± 2.2 ng.mL^{-1}.

Resumo

Este trabalho tem como objectivo a optimização de condições de produção do Factor Inibitório da Leucemia (hLIF, do inglês "Leukemia Inhibitory Factor") através da linha celular de rim embrionário humano 293 (HEK293, do inglês "human embryonic kidney 293") - EBNA1 cultivada sob a forma de agregados em suspensão em frasco agitado. Foram estudados os efeitos da densidade inicial de inóculo celular e regime de alimentação no crescimento e produtividade.

Uma primeira fase decorre até ao final do crescimento exponencial em meio suplementado com soro, seguindo-se de uma selecção por puromicina para as células portadoras do plasmídeo com hLIF. A segunda fase, de produção, decorre em meio sem soro. São testadas três densidades de inóculo (2×10^4 células.mL^{-1}, 2×10^5 células.mL^{-1} e 2×10^6 células.mL^{-1}) de modo a avaliar a sua capacidade de expansão celular e distribuição dos tamanhos dos agregados celulares. O inóculo de 2×10^5 células.mL^{-1} permitiu a obtenção de uma concentração celular final de aproximadamente 7×10^6 células.mL^{-1} e agregados celulares homogéneos com cerca de 278 μm. O efeito do regime de alimentação foi estudado na produção de hLIF recombinado para a densidade de inóculo de 2×10^5 células.ml^{-1}, através da análise de metabolitos.

A analise de metabolitos revelou o esgotamento de glucose e glutamina após 9 e 7 dias, respectivamente, no regime da alimntação de 25%. Assim, a glutamina actua como fonte de carbono, energia e aminoácidos alternativa no crescimento das células HEK293-EBNA1. Os níveis de lactato observados foram abaixo das concentrações inibitórias (30 mM [1]). Aparentemente, as células HEK293-EBNA1 não foram afectadas pelos níveis de amónia produzidos.

Em conclusão, o regime de alimentação de 25% no inóculo de 2×10^5 células.mL^{-1} obteve as mais elevadas densidades celulares, tanto durante o tempo de cultura relativo ao crescimento como à fase de produção, com agregados em suspensão abaixo do tamanho de necrose. Estes condições permitiram alcançar a produtividade volumétrica de hLIF mais elevada, 125 ± 2,2 ng.mL^{-1}.

Keywords

human embryonic kidney 293 (HEK293) cells

leukemia inhibitory factor (LIF)

feeding regimen

cell density

cellular aggregate-size distribution

nutrient metabolism

Index

List of Figures

List of Tables

List of Abbreviations

aa	amino acid
ADP	adenosine di-phosphate
ATP	adenosine tri-phosphate
bFGF	basic fibroblast growth factor
BHK	baby hamster kidney
BMP-4	bone morphogenetic protein- 4
CHO	chinese hamster ovary
CIRP	cold-inducible RNA-binding protein
CMV	cytomegalovirus
CO2	carbon dioxide
COS	Acronym derived from the cells being CV-1 (simian) in Origin, and carrying the SV40 genetic material
DMEM	Dulbecco's Modified Eagle Medium
DNA	Deoxyribonucleic acid
EBNA1	Epstein-Barr virus nuclear antigen 1
EBV	Epstein-Barr virus
EGF	Epidermal growth factor
ELISA	Enzyme Linked Immuno-Sorbent Assay
EPO	Erythropoietin
ES	embryonic stem
FI	Fold Increase
FR	Feeding Regimen
FBS	Fetal Bovine Serum
FGF2	Fibroblast Growth Factor 2
gpl30	Glycoprotein 130
H_2O	water
hASCs	human adipose-derived stromal/stem cells
HEK293	human embryonic kidney
HGF	hepatocyte growth factor
hLIF	human LIF
IL-6	Interleukin-6
K+	potassium
LC-SFM	vascular endothelial growth factor
LDH-A	lactate dehydrogenase-A
LIF	Leukemia Inhibitory Factor
LIFRβ	LIF-specific receptor subunit β
Na^+	sodium
NH_3	ammonia
NH_4^+	ammonium
O2	oxygen
PDB	Protein Data Bank
q_{amm}	Specific ammonia production rate
q_{glc}	Specific glucose consumption rate
q_{gln}	Specific glutamine consumption rate
q_{lac}	Specific lactate production rate
Ras/ERK	*Ras*/*ERK* signaling cascade - transduction pathway
rCHO	recombinant chinese hamster ovary
r-proteins	recombinant proteins
SDS-PAGE	sodium dodecyl-sulfate polyacrylamide gel electrophoresis
STAT3	signal transducer and activator of transcription 3
SV40	Simian vacuolating virus 40 or Simian virus 40
TCA	tricarboxylic acid

TGE	transient gene expression
tPa	tissue Plasminogen activator
VEGF	vascular endothelial growth factor
$Y'_{amm/glut}$	Ammonium / glutamin yield
$Y'_{lac/glu}$	Lactate / glucose yield
μ_{max}	maximum growth rate

Part of the work developed in this thesis was previously presented in the poster:

RICARDO P. BAPTISTA, **DAVID M. BARATA**, LUÍS P. FONSECA, MARGARIDA M. DIODO, CLAUDIA LOBATO DA SILVA, JOAQUIM M. S. CABRAL. ***Production of human Leukemia Inhibitory Factor (LIF) in a mammalian cell bioreactor.*** 4th International Meeting of the Portuguese Society for Stem Cells and Cell Therapies (2009)

1. Introduction

Over the past two decades, biopharmaceuticals like recombinant proteins (r-proteins) have gained increasing importance for therapeutic applications. The overall number of proteins either approved or launched into clinical trials has continually increased over this period, representing an annual global market that is now valued to be more than 34 billion € with an annual sales increase of about 20%. Currently, about 60% of all recombinant therapeutic proteins are produced in mammalian cell systems, due to the ability of mammalian hosts to generate high-quality proteins that are similar in their biochemical properties to the naturally occurring forms [2]. This growing demand for high-quality recombinant therapeutics is driving the research and development of mammalian-cell-based technological systems for enhanced production yields.

In 1997, sales of biotherapeutics produced by cell culture were 2.2 billion € whereas *E. coli* based biotherapeutics amounted to 1.8 billion € [3]. By 2006, production of therapeutic proteins by mammalian systems reached 14 billion € [4].

(original currencies in USA dollar, converted to Euro in November 2009)

1.1. Animal cells and Recombinant Proteins

One major advantage of using mammalian cells in protein production is directly related to the correct assembling and folding of recombinant polypeptides, as well as additional critical post-translational modifications, that are usually strictly required for biological activity [5]. Most proteins are indeed glycosylated, and all these glycosylations from the single sugar to the many branched or linear chains, exhibiting particular *O*- or *N*-linkage [6, 7], have consequently made r-proteins more complex to engineer than initially thought. As an example, the appropriate glycosylation of recombinant erythropoietin (EPO), which has been approved as a drug for anaemia and cancer, has been shown to be critical for its activity and longevity of action [8]. However, there are many examples where therapeutic products have failed in clinics because of their defective glycolysation processing [9]. Many early attempts at introducing protein therapeutic molecules failed because the protein drug molecules were recognised as nonhuman and led to an immune response against the drug itself. As a result, most proteins used in clinical trials now are primarily human or are humanised, even if the original ‘proof of concept’ work was done with nonhuman proteins. The

immunogenicity of mouse antibodies in humans was one of the major reasons why early monoclonal antibodies did not deliver the anticipated therapeutic benefits [10].

Mammalian cell cultures are particularly useful because the proteins are often made in a properly folded and glycosylated form, thus eliminating the need to renature them. Eukaryotic cells are also useful for addition of fatty acid chains and for phosphorylating tyrosine, threonine and serine hydroxyl groups [11].

In contrast to lower eukaryotes or prokaryotes, mammalian cells provide active r-proteins that possess relevant post-translational modifications. Even if necessary glycosylation for stability or proper folding (e.g. EPO and human chorionic gonadotropin) can often be provided by recombinant yeast, mold, insect or mammalian cells, only mammalian secreted proteins are properly glycosylated with *D*-mannose sugars covalently bound to asparagine-linked *N*-acetyl-*D*-glucosamine molecules [12]. Although fungal excreted enzymes often show the same type of glycosylation [13], sometimes additional carbohydrates linked to the oxygen of serine or threonine are present in fungal proteins [14]. Glycosylation also affects pharmacokinetics (residence time in vivo) [15]. Other modifications, can as well confer stability enhancement against proteolytic attack like terminal sialic acid addition on EPO [16], human tissue plasminogen activator (tPa) [17] and interferons [18] (with regard to activity, human EPO is 1000-fold more active *in vivo* than its desialylated form but they both have similar *in vitro* activities [19]

Mammalian cells have have high productivities of 20-60 $pg.cell^{-1}.day^{-1}$ of recombinant protein. tPa was produced in *Chinese Hamster Ovary* (CHO) cells at 34 $mg.L^{-1}$ with an overall yield of 47%. Although production in *E. coli* was at a much higher level (460 $mg.L^{-1}$), recovery was only 2.8% due to production as inclusion bodies and low renaturation yields [20]. r-protein production in mammalian cells rose from 50 $mg.L^{-1}$, in 1986, to 4.7 $g.L^{-1}$, in 2004, mainly due to media improvements yielding increased growth [21]. A titre of 2.5-3 $g.L^{-1}$ protein in 14 day CHO fed-batch shake flask culture was achieved using $Fe_2(SeO_3)_3$ as ionic carrier [22]. A number of mammalian processes are producing 3-5 $g.L^{-1}$ and, in some cases, protein titres have reached 10 $g.L^{-1}$ in industry [23]. A rather new system uses a human cell line known as PER.C6 of Crucell Holland BV, which, in cooperation with DSM Biologics, was reported to produce 15 $g.L^{-1}$ [24] and then later, 26 $g.L^{-1}$ of a monoclonal antibody [25].

Significant improvements have been made in r-protein volumetric and specific productivities, in great part due to the increase of cell viability and maintenance in

culture for long term. Cell growth in standard production culture systems can be divided into four phases, i.e. lag, exponential, stationary and decline or death phase.

Long lag phases are undesirable, therefore high growth rates are essential at the beginning of a process to achieve enough cells in order to maximize the production of the desired bio-product. Uncontrolled proliferation beyond a certain desired cell density is also undesirable due to nutrient and oxygen depletion, toxic metabolite accumulation, cell death, and degradation of the product [26-28]. In Figure 1.1 is represented the effect of engineered rCHO cells for improved culture characteristics, resulting in an enhanced lifespan and production.

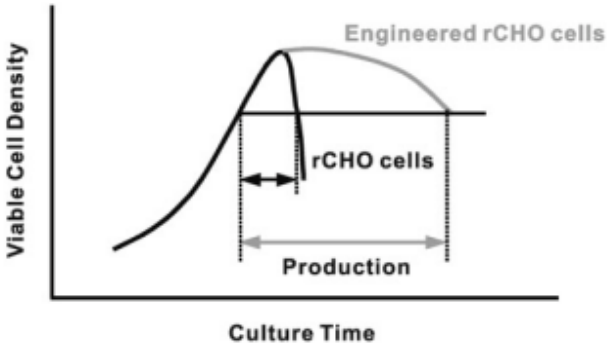

Figure 1.1 – Schematic depiction of the effect of engineering rCHO cells for improved culture characteristics. Engineering rCHO cells results in the enhancement of culture longevity, which reflects on the production titre. Adapted from *Mohan et al* [29].

Proliferation control strategies are typically implemented in the mid- or late-phases of exponential growth and have been shown to improve both the productivity and duration of production processes. If cell engineering is not used in conjunction with the right conditions, no significant improvement in protein production is achieved. Strategies to extend culture longevity could be tried, such as overexpression of anti-apoptotic genes, down-regulation of apoptotic effector molecules, overexpression of pyruvate carboxylase, down-regulation of lactate dehydrogenase-A (LDH-A), and down-regulation of cold-inducible RNA-binding protein (CIRP) [29].

Medium composition, especially serum components, affects the concentration of autocrine signalling factors determinant of growth [30, 31] that could seriously have an important role in culture kinetics.

Several factors were identified to affect the proliferative capacities in different tissues, namely the vascular endothelial growth factor (VEGF), the hepatocyte growth factor (HGF), and the basic fibroblast growth factor (bFGF) [32-35]. More recently, *Herbert et al* [36] reported that human adipose-derived stromal/stem cells (hASCs) *in vitro* cells supplemented with EGF and bFGF significantly increased proliferation by up to three-fold over 7-8 days.

1.2. Medium formulation

Although serum is a common component of culture medium containing a set of important nutrients and other elements as anti-apoptotic factors that protect cells from apoptosis [37], strict regulatory requirements restrict the use of serum- or protein-free media for the large-scale culture of cells. Hence strategies have been developed to fulfil these requirements. The apoptosis modulation is a variable intensively studied and several strategies have been proposed, like the manipulation of external cellular environment through media supplementation or by manipulation of intracellular environment using genetic engineering [29]. Serum-free suspension processes are often the preferred mode for the production of animal recombinant proteins due to its easy in scale-up process and operation, simplicity in downstream processing and reduced risk of virus contamination.

A major allocation of resources in culture lifespan enhancements has been used for anti-apoptosis cell engineering to tackle the problem of programmed cell death occurring under stressful conditions. Several studies have already demonstrated the successful adaptation of *Human Embryonic Kidney* cells (HEK293) cells growth in serum-free, keeping the protein quality [1, 38]. Even though serum is a cell protector that increases cell viability and proliferation [27, 37], new formulations must be developed to provide less complex feedstream for downstream processing and allow improvements in r-protein yields.

1.3. Cell metabolism

Glucose and glutamine are the main nutrients of animal cells and both can interchangeably be used as energy sources. Glucose is either utilized trough the pentose phosphate pathway to supply nucleotides for biosynthesis [39, 40] or through the glycolysis pathway to provide metabolic intermediates, such as pyruvate, and energy. Pyruvate is preferably converted to lactate and fatty acids, but it can also become oxidized in the tricarboxylic acid (TCA) cycle [41, 42] originating H_2O and CO_2, followed by the formation of high-energy phosphate bonds by phosphorylation of ADP to ATP (coupled to the transfer of electrons from reduced coenzymes to molecular oxygen) via the electron transport chain. On the other hand, glutamine is oxidized to CO_2 and is a key aminoacid, since it is consumed at a higher rate than other amino acids [43]. Glutamine can be used to produce other amino acids or to be incorporated into the biomass; however the majority is converted to glutamate. Then glutamate can be converted to α-ketoglutarate and enter the TCA via one of the two next pathways: production of alanine or by a more efficient process that results in the production of an additional molecule of ammonia [44].Also the overall amino acids in media composition is important in product formation

Within these catabolic pathways, comparable for different animal cell types [45-48], lactate and ammonia are presented as major metabolic waste products, to an extent that is specific for each cell line [49], due to the different sensitivities of key enzymes in the glucose and glutamine metabolic pathways and respective shifts in response to the environment signals. Glucose and glutamine metabolism is resumed in Figure 1.2 (more details for each molecule catabolism are presented in Appendix, 6.1).

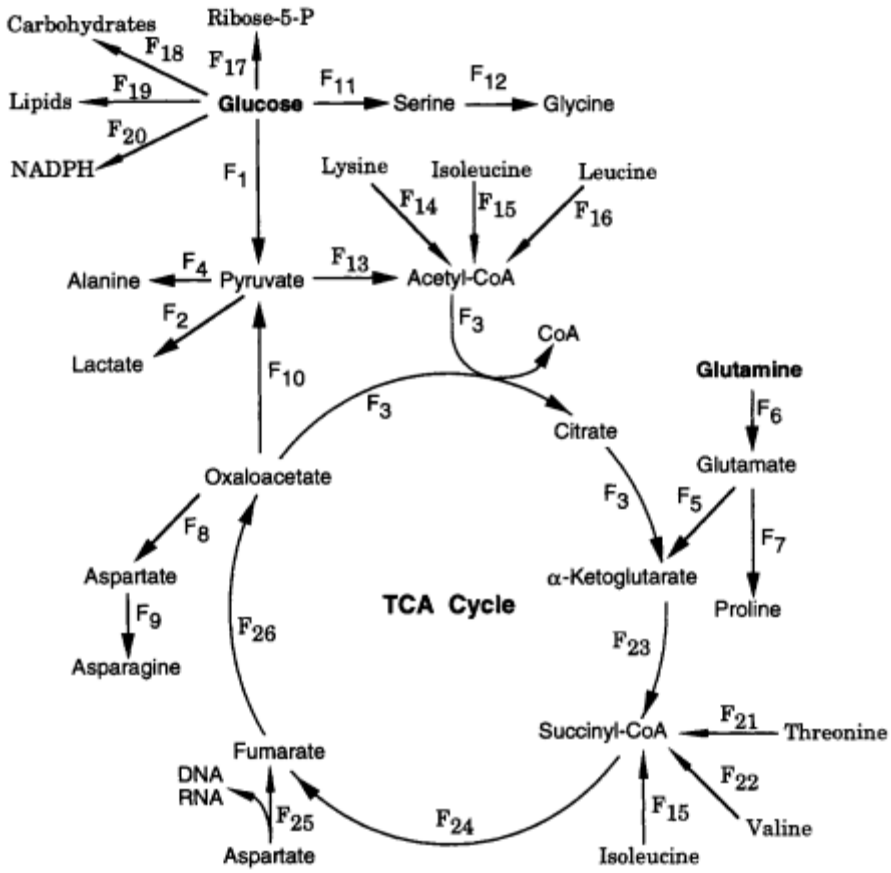

Figure 1.2 – Schematic diagram of simplified reaction network for animal cell metabolism. F1 to F26 are respective to mediating enzymes involved in the metabolism. Adapted from Xie and Wang [50]

Considering metabolic engineering as a tool to overcome these limitations [29], indirect increases in cell growth and volumetric production had been achieved, mainly by inhibiting the accumulation of these toxic metabolic by-products, lactate and ammonium, which showed significant results. The strategies are generally based on:

- reducing the accumulation of lactate in cell culture media; lactate accumulation acidifies the medium and hence requires the addition of more base (increasing the osmolality and adversely affecting the cell growth and product quality);
- improving the efficiency of the primary metabolism, by redirecting cells into pathways using energy more efficiently.

Some examples can be the LDH-A knock out (reducing glucose consumption rate, thus reducing lactate production) within normal proliferation kinetics [51], the overexpression of urea cycle enzymes like carbamoyl phosphate synthase and ornithine transcarbamoylase (reducing accumulation of ammonia ions) [52], or the overexpression of pyruvate carboxylase to increase glucose flux into the tricarboxylic acid cycle [53].

These examples demonstrate the potential to overcome, in large-scale production of recombinant heterologous proteins, toxic metabolic by-product accumulation, inhibitors of cell growth.

1.4. Systems for Recombinant Protein Expression

Traditionally, in order to obtain sufficient amounts of protein for structure and biological activity analysis in high-throughput screenings, one needs to go to through the long, costly and time-consumption process of stable transfectoma isolation and characterization [54, 55].

Gene expression by large-scale transfection of mammalian cells is becoming an established technology for the fast production of r-proteins. However, efforts are still needed to optimize production parameters in order to maximize productivities while maintaining product quality [56].

Until 2001, transient gene expression (TGE) have been exploited only for the synthesis of smaller quantities of r-proteins using different cell lines, e.g., COS[1] cells [57], HEK293 [58], and *Baby Hamster Kidney* (BHK) cells [59]. However, this technique has recently begun spreading to a large-scale as a powerful technology to generate large amounts of r-proteins within a few days [54, 55, 59-64].

Moderate quantities (1-500 mg) of complex r-proteins for functional and structural analysis [65, 66] can now be easily obtained through TGE in animal cells, mostly because of its cost-effectiveness and speed compared to the time-consuming and laborious establishment of stable cell clones [59]. Furthermore, when a large number of different proteins or variants of the same protein need to be tested, the transient system can be efficiently applied in a high-throughput approach for parallel evaluation [54, 67].

[1] COS is an acronym, derived from the cells being **C**V-1 (simian) in **O**rigin, and carrying the **S**V40 genetic material

For an optimal large-scale transient transfection and r-protein expression on mammalian cells, four key aspects need to be taken into account, namely:

- the cell line;
- the expression vector;
- the transfection vehicle;
- the culture medium.

The human embryonic kidney 293, HEK293 [68] cell line, and the subclone 293 expressing the Epstein-Barr virus (EBV) nuclear antigen 1 (EBNA1) cell lines, became important for production of viral vectors for gene therapy and also for expression of r-proteins, e.g. using extra chromosomal EBV based vectors [69]. The HEK293(EBNA1) expression system exhibits many advantages compared to CHO or BHK systems. For example, it is of human origin, it exhibits high transfection efficiency, have autonomous replicating vectors available, it is useful for expressing human proteins and, finally, the cells are relatively easy to grow in serum-free suspension culture [70, 71]. Moreover, two genetic variants, the 293E and the 293T cell lines, expressing the EBNA1 or the SV40 large-T antigen, respectively, allow episomal amplification of plasmids containing the viral EBV (293E) or SV40 (293T) origins of replication. Thus, they are expected to increase r-protein expression levels by permitting more plasmid copies to persist in the transfected cells throughout the production phase [72].The second important issue for high level r-protein expression is to use vectors with promoters that are highly active in the host cell line, such as the human cytomegalovirus (CMV) promoter [73]. This promoter is particularly powerful in HEK293 cells where it has been shown to be strongly transactivated by the constitutively expressed adenovirus E1a protein [74]. A highly efficient expression cassette using this promoter was recently described that provides adenovirus-mediated transgene expression levels reaching up to 20% of total cell proteins [75, 76]. HEK293-EBNA1 cells and *oriP* plasmid constitute a powerful transient expression system in which the episomal replication of plasmid is initiated by EBNA1 binding to *oriP* [77]. HEK293-EBNA1 expression system is schematically represented in Figure 1.3. Transfection productivity should be considered together with the cell construct when evaluating productivities.

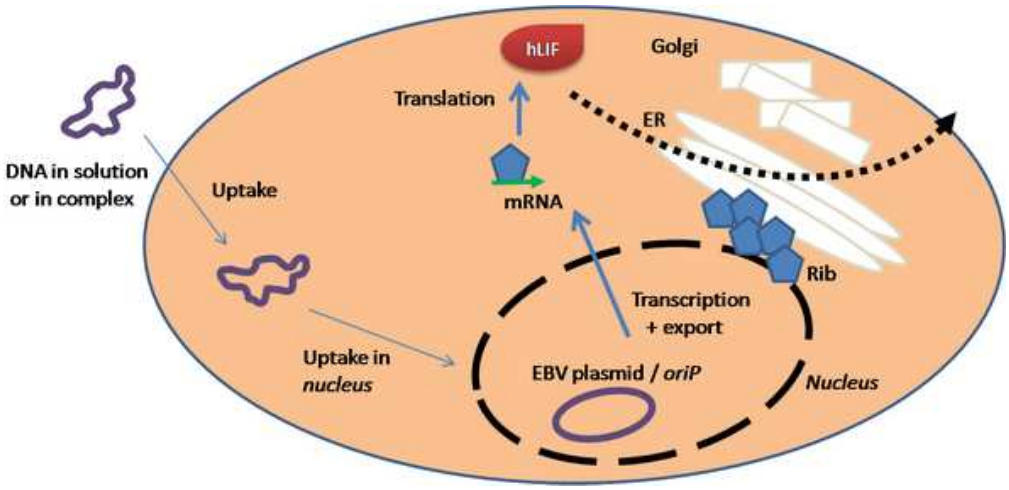

Figure 1.3 – Schematic representation of the HEK293-EBNA1 transient expression system. The plasmid is inserted into cell, migrating to nucleus, where the target sequence is transcript and subsequently expressed as peptide by cytoplasm machinery, processed and secreted.

Durocher el al formulated an *oriP* plasmid pTT, derived from a commercially available pCEP4, which was able to enhance expression of protein by several folds [54]. The third aspect is related to gene transfer reagent efficacy. Even though many highly effective gene transfer reagents are commercially available, only a few are cost effective when considering operations at the multi-litre scale.

There are several advantages of episomal vectors: first, the inserted gene of interest cannot be interrupted or subjected to regulatory constraints, which often occur from integration into cellular DNA. Secondly, the presence of the inserted heterologous gene does not lead to rearrangement or interruption of the cell's own important regions. Thirdly, episomal vectors persist in multiple copies in the nucleus, resulting in amplification of the gene of interest, whenever the necessary viral trans-acting factors are supplied [72]. Finally, in stable transfection procedures, the use of episomal vectors often results in higher transfection efficiency than the use of chromosome-integrating plasmids [78, 79]. Furthermore, episomal vectors are plasmid constructions that replicate in both eukaryotic and prokaryotic cells and can therefore easily be “shuttled” from one cell system to another. This feature and the fact that some episomal vectors can transfer large amounts of DNA allow applications, such as screening of cDNA libraries [80-82]. Episomal vectors recur to cellular enzymes for replication and repair, being powerful tools for studying DNA replication or mutagenesis [83, 84].

The stability of the episomal vectors might be questioned, but it does not seem to be critical. As reviewed by *Van Craenenbroeck et al.* [72], *oriP* and EBNA1 are the only viral elements necessary and sufficient for stable episomal maintenance of viral DNA in the cell. This stable episomal maintenance reflects the sum of plasmid replication and efficient segregation to the daughter cells. The better understanding of this cell line would be an advantage, once that HEK293, as well as CHO, are the preferred cells to TGE owing to their high transfectability and the ability of these cells to support high-density in growth in suspension [55, 85].

1.5. Culture systems

Depending on the nature of cells in culture, if they are anchorage-dependent or if they grow in suspension, some culture systems are available for laboratorial and industrial scale, as shown in Figure 1.4. There are numerous immobilization options for cell adhesion and retention in suspension cultures, like microcarriers, being possible to scale-up [86, 87], but with the disadvantage of being more expensive than culture as aggregates.

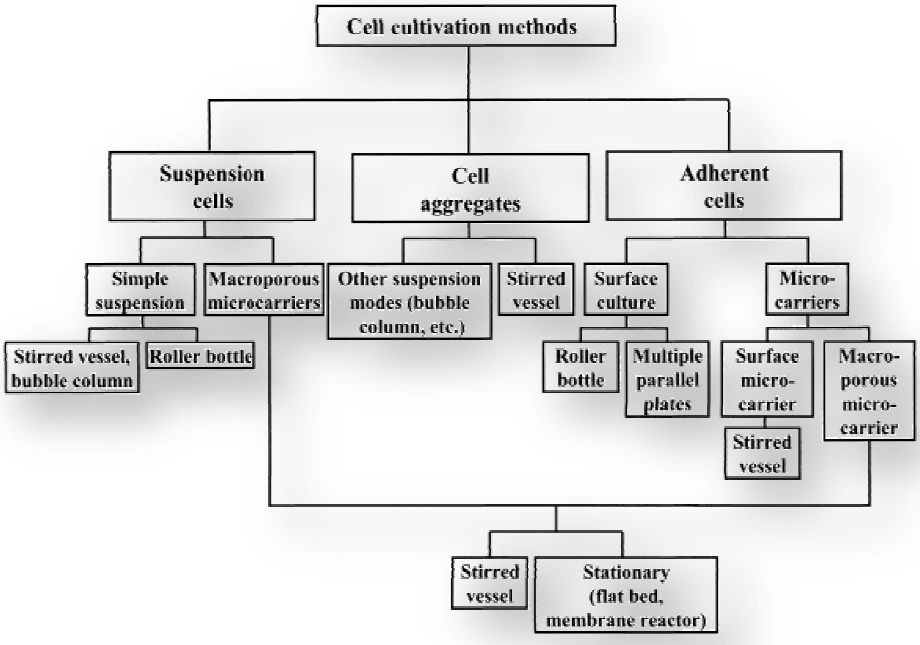

Figure 1.4 – Cell cultivation methods applicable for expansion and differentiation of stem cells. Adapted from *Ulloa-Montoya et al.* [88]

The HEK293 cell line was adapted to growth in suspension [70], forming cell aggregates as a self-immobilization strategy, as presented in Figure 1.5. This can be considered as an alternative approach to producing bioactive cellular products [89-91]. Whereas in perfusion culture systems more complex strategies must be adopted to perform cell retention (as spin filters and others) [92], in fed-batch systems, cell sedimentation can be easily used regarding medium change. HEK293 cells were already setup until 100 litre scale transient transfection in a standard stirred bioreactor, demonstrating not only the scale-up availability of cellular aggregates suspension, but also the robustness of large scale transient gene expression [64].

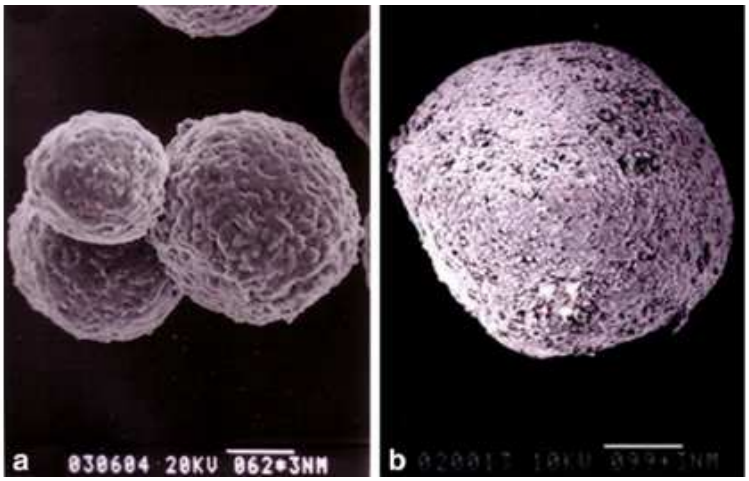

Figure 1.5 – Scanning electron microscopic observations of the HEK 293 cell aggregates in perfusion culture. a) 5 days after inoculation, b) 17 days after inoculation. The scale bars in a) and b) indicate 62 and 99 μm, respectively. Adapted from *Liu et al.* [93].

Suspended mammalian cell cultures are normally cultivated in glass or stainless-steel stirred tank bioreactors, properly designed with impellers that minimize shear forces [94]. These bioreactors can be operated in three different modes, including batch, fed-batch, or perfusion, where each one has its advantages and disadvantages [95]. Homogenous perfusion mode is usually known by achieving higher cell density and productivity than either the batch or fed-batch designs, in relatively small volumes. In perfusion mode, high cell number and productivity, as well as steady supply of nutrients and continuous removal of metabolic by-products must follow the growth kinetics and production phase. Perfusion is also characterized by a medium dilution rate exceeding that of cellular growth, needing a dependable separation approach to retain cells in the bioreactor. In batch or fed-batch, the metabolite removal is not fully supported, being a limitation overcame in a perfusion design.

In laboratory scale, spinner flasks, simple stirred vessels, operating as fed-batch cultures are a simple and economic way to study basic parameters before undergo scale-up strategies at higher volumes. Their relatively homogenous nature makes them uniquely suited for investigations of different culture parameters (e.g. dissolved O_2, pH, temperature, agitation rate, serum components medium exchange rates, etc) that may influence the viability and turnover of cells in culture [42, 96]. Another important parameter to control is the particle size and their density in suspension, because it must be considered for large-scale cell retention [92] during feeding and other operations.

Agitation rate is also an important variable to consider in suspension stirred culture. Despite the high agitation rate promotes frequent collisions between cells or cells and microcarriers favouring proliferation and avoiding sedimentation, this could be a critical factor to consider in terms of hydrodynamic shear stress, because higher stirring velocities may affect cell membrane integrity, as well as cell function [97]. In order to better control the culture environment, to minimize shear stress and bursting bubbles, some authors have studied the possibility of add protective agents such as surfactants (and also serum, which besides its nutritional role, has some cell protective effects, despite the technical disadvantages of its use, as previously mentioned) [98].

1.6. Leukemia Inhibitory Factor

The Leukemia Inhibitory Factor (LIF) is a variably glycosylated, 38-67 kDa polypeptide originally identified as a proliferation inhibitor and differentiation inducer of the mouse M1 myeloid leukemia cell line [99-101]. The mature LIF molecule measures 179 amino acid (aa) residues in length with multiple potential *N*-linked and *O*-linked glycosylation sites plus six conserved cysteines that form three intramolecular disulfide bridges. Mature mouse LIF is 78% identical to human LIF at the aa sequence level [102, 103]. The tertiary structure of human LIF (hLIF) is presented in Figure 1.6.

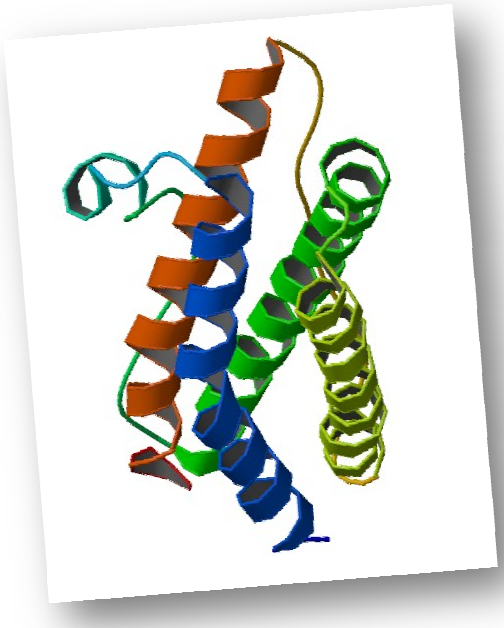

Figure 1.6 – 3D structure of human Leukemina Inhibitory Factor (PDB entry *1emr*)

LIF appears to be a generalized stem cell factor as many of its actions are mediated via stem cells or progenitor cells rather than by a direct effect on differentiated tissues [104, 105]. For example, LIF-deficient mice have dramatically reduced numbers of stem cells in spleen and bone marrow [106]. Receptors for LIF are present on cells of monocytic series, embryonic stem cells, embryonic carcinoma cells, on a majority of lymphocytes, myoblasts, hepatocytes, osteoblasts, adipocytes and adrenal cortical cells [107]. Partially, the transduction mechanism of LIF on these cells is shared by Interleukin-6 (IL-6) [108] which also uses gpl30 for signal transduction [109] and triggers the same immediate early response during induced differentiation of murine leukemic cells [110]. The mechanism of action of LIF is presented schematically in Figure 1.7. An association of LIF with its heterodimeric receptor, which consists on a LIF-specific receptor subunit β (LIFRβ) and IL-6 signal transducer gp130, results in the activation of several intracellular signalling pathways, including the signal transducer and activator of transcription 3 (STAT3) pathway, the Ras/ERK pathway and the PI3 kinase pathway [111]. However, the differentiation inhibitory effect of LIF on embryonic stem cells is not shared by IL-6 class cytokines.

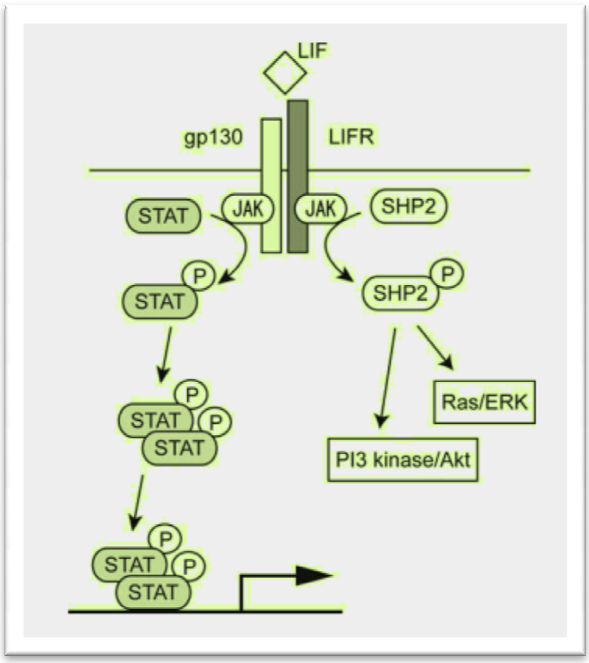

Figure 1.7 – Intracellular signaling pathways activated by LIF. Adapted from *Okita et al* [111].

The cytokine LIF and its downstream effector STAT3 are essential for maintenance of pluripotency in mouse embryonic stem cells. The requirement for the transcription factor Oct3/4 for embryonic stem cells (ES) cell pluripotency is also well documented. However, LIF is not involved in self-renewal of human ES cells, suggesting that other pathways must play an important role in this process. The importance of other signal transduction pathways, including BMP (bone morphogenetic protein) and Wnt signalings, as well as novel transcription factors such as Nanog, is now being recognized [111]. Figure 1.8 briefly overviews the complexity of signals involved in the intracellular signalling pathways that contribute to self-renewal of pluripotent mouse and human ES cells.

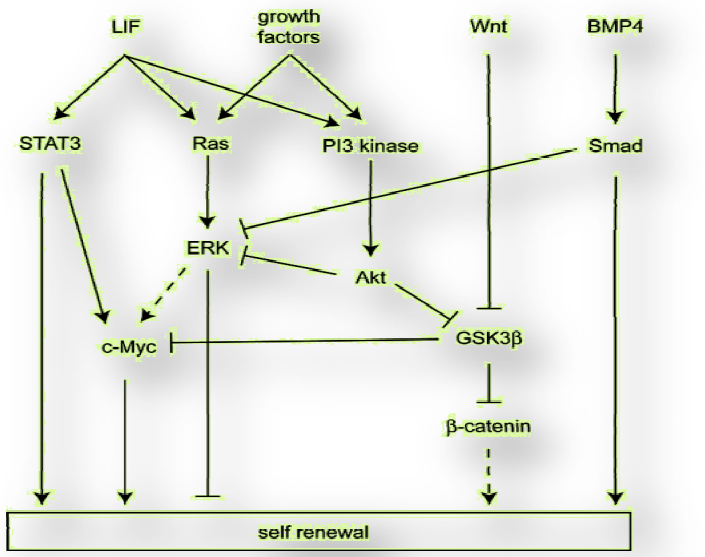

Figure 1.8 – Potential crosstalk between intracellular signalling pathways in mouse ES cells.
Adapted from *Okita et al* [111].

About LIF action in the organism development, it is known that:

- it can inhibit the growth and induce macrophagic differentiation in murine leukemic M1 cells [112], while preventing the differentiation in normal totipotential embryonic stem cells [113];

- it inhibits the induced differentiation of mouse F9 [114] and P19 embryonal carcinoma cells [115] selectively inhibiting the formation of primitive ectoderm, while permit the differentiation of primitive endoderm [116];

- during embryonic development, LIF is expressed in blastocyst and in egg cylinder [106] and might play a crucial role in implantation process [117].

Overall, the establishment of an effective and reproducible platform for the production of hLIF will allow to produce large amounts of a well-defined product *in house*, avoiding the need to acquire large amounts of this costly product (as other cytokines/growth factors) to commercial sources. Moreover, this platform can be easily adapted for the production of other cytokines/growth factors to be used in stem cell culture, but also molecules with a therapeutic potential in clinical settings.

2. Methods

2.1. Cell line

HEK293-EBNA1 cells were a kind gift from W. Mueller and M. Hafner, GBF, Braunschweig – Germany. These cells were previously transfected and contain copies of a pCMV plasmid encoding for human Leukemia Inhibitory Factor (hLIF) and containing a resistance marker for purymicin. HEK293-EBNA1 cells were kept frozen at – 80 ºC until further use.

2.2. HEK293 expansion in static conditions

HEK293 were passed routinely and expanded as adherent monolayer cultures in T-flasks (75 cm^2) at 37 °C in a humidified 5% CO_2 atmosphere. Cells were cultivated in Dulbecco's modified Eagle's medium (DMEM, glucose at 22 mM) supplemented with 10% (v/v) fetal bovine serum (FBS) (Gibco®), 1% (v/v) penicillin (50 U/mL)/streptomycin (50 U/mL) (Gibco®) and 1% glutamine 200 mM (Gibco®). Trypsinization was performed using a 0.25% (w/v) trypsin-phosphate buffered saline (trypsin/PBS) solution, and the cells were passaged every 4–5 days (confluence of 80-90%) at a seeding density of 2×10^5 cells.mL^{-1} in T-flasks of 75 cm^2. In each passage, cell viability was determined in a hemocytometer using the trypan blue dye exclusion test under an optical microscope (Olympus CK40).

2.3. HEK293 expansion under dynamic conditions

2.3.1. Spinner flask culture system

HEK293 expansion was performed in 100 mL spinner flasks where the cells were able to grow in suspension as aggregates (Figure 2.1). The spinner flask is equipped with an impeller with 90º normal paddles (Flat Bottom Adjustable Hanging Bar Spinner Flask Complete – 100mL, from Bellco®) and a magnetic stir bar. The

glass surface of the spinner flask was siliconized (Sigmacote, Sigma) in order to prevent the adhesion of cells and aggregates to the glass walls. Before and after use for cell culture, spinner flasks were washed with Milli-Q ® water and sterilized by autoclaving.

Figure 2.1 – Spinner flasks used for HEK293 culture, from Bellco®

Cells were grown at 37° C in a 5 % CO_2 humidified atmosphere and replenished daily with fresh medium beginning on the third day of the culture. Agitation rate was set at 80 rpm, value previously optimized at BERG/IBB-IST.

2.3.2. Feeding regime

Spinner flask medium was replaced in function of the chosen feeding regime, changed on a daily routine starting on the second day of culture growth. Three feeding regimen were tested: 25%, 50% and 75%, either in the initial cell density of 2×10^5 cells.mL^{-1} and 2×10^6 cells.mL^{-1}. Each time, medium was removed after a simple step of sedimentation of 30-40 minutes, being replaced by fresh sterile medium, in the fraction according with the feeding regime in order to keep a constant final volume of 100 mL.

2.3.3. Sampling

Duplicate samples of 1 ml of evenly mixed culture were taken every day. Samples were centrifuged at 1500 rpm for 3 minutes. Cells were ressuspended for 5 minutes at 37º C with half of initial volume of a 0.25% trypsin solution (1% when

occurring larger aggregates than 150 μm), followed by addition of ½ of initial volume of medium (with FBS) to stop enzymatic activity. Cells were then ressuspended for counting viable and dead cells in suspension using the trypan blue exclusion method. The supernatants were kept at -20º C for metabolite analysis.

Cell viability across experiments and trypan blue exclusion method robustness was tested, as presented in Appendix, 6.2.

2.3.4. Aggregate-size distribution assay

The average diameter of the HEK293 cell aggregates in the spinner flasks was determined by optical analysis of 10 to 20 aggregates (essentially spherical in shape) recurring to a graduated ocular lens (Olympus NCWHK10X) on a optical microscope (Olympus CK40). Images were obtained directly from an eyepiece reticule and one inverted light microscope (Leica DMI 3000B) using Nikon® Act-1 analysis software.

2.3.5. Data analysis

The growth kinetics of HEK293 cells cultured under stirred conditions on microcarriers was also characterized. Specific growth rates were calculated according to Equation 2.1, from *Melero-Martin et al.* [118]:

$$\mu = \frac{1}{X}\frac{dX}{dt} \approx \frac{2}{X_2 + X_1}\frac{X_2 - X_1}{t_2 - t_1} \quad (2.1)$$

where μ (day^{-1}) corresponds to the value of specific growth rate at any given time point, t (days) the culture time and X (cells) the value of viable cell number for a specific t. From this, the doubling time (t_d) was calculated using the following Equation 2.2,

$$t_d = \ln(2)/\mu_{max} \quad (2.2)$$

For a more rigorous calculation of μ_{max}, a curve fitting was calculated using Origin® software (under a test licence) within a 100 points non linear regression, using Logistic function, in order to reduce operator and sampling variability. This simulation data was plotted in Microsoft Excel and a linear regression was obtained for the exponential phase of growth, where the μ_{max} is obtained by the slope (m) in the linear regression equation: $y = m.x + b$ (see Appendix, 6.3).

2.3.6. Lactate Dehydrogenase activity

Lactate dehydrogenase (LDH) is an enzyme present in the cells that catalyses the interconversion of pyruvate and lactate. The activity of this enzyme is a quantitative measurement of loss of cell viability as dead or dying cells release this enzyme. For determination of LDH activity levels during time in culture, a LDH analysis kit from Promega was used (CytoTox96 non-radioactive cytotoxicity assay). A calibration curve using several dilutions of cells, which were submitted to lysis, was performed according to manufacturer's instructions. This test was used to confirm the accuracy of trypan blue assay in measuring dead cell number (see Appendix, 6.2).

2.4. Determination of metabolite profiles during time in culture

Glucose, lactate, glutamine and ammonia concentrations were determined in the supernatant samples collected throughout the experiments by using an automatic analyzer (YSI 7100MBS, Yellow Springs Instruments). The specific metabolic rates ($q_{Met.}$, mol.10^6 cells.h^{-1}) were calculated for every time interval using the following equation: $q_{Met.} = \Delta Met./(\Delta t.\overline{Xv})$, where ΔMet. is the variation in metabolite concentration during the time period Δt and ΔX_v the average viable cell number during the same time period. The apparent lactate from glucose ($Y'_{lac/glu}$) yield was also calculated as the ratio between q_{lac} and q_{glu}

2.5. Recombinant hLIF expression analysis

2.5.1. Cell selection at production phase in static culture

For hLIF expression, after becoming confluent, cells were split into another flash where puromycin (Invitrogen®) at 0.5 mg.mL^{-1} was added. Then, after 3 days (with

cells confluent), cells were spliced and cultured with medium without puromycin. After 3 more days, the medium was changed by medium without FBS. The final supernatant was collected after 2 days and filtered through a 0.2 μm filter, before being stored at – 20 ºC. The protocol can be schematically described by Figure 2.2.

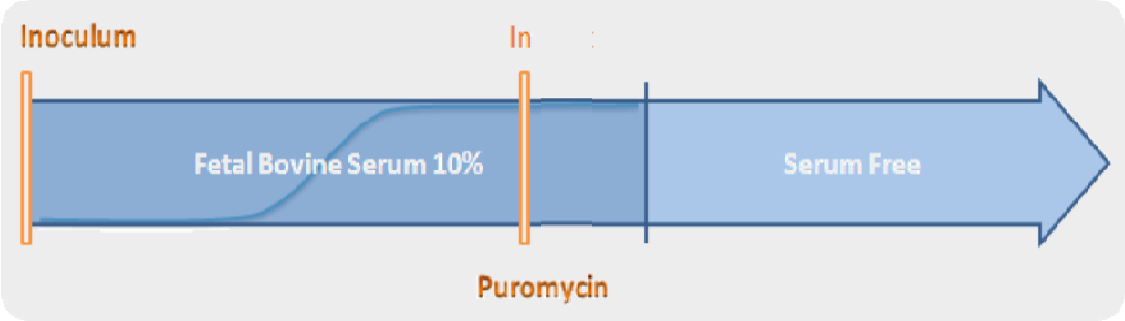

Figure 2.2 – HEK293-EBNA1 growth evolution timeline, selection and production phase under serum-free conditions

2.5.2. Cell selection at production phase in spinner flask culture

HEK293 cells containing the hLIF plasmid where selected by puromycin resistance at steady phase. Puromycin was added to culture at 0.5 $mg.mL^{-1}$ and diluted 24 hours later by two new media replenishments of 50% of volume, preceded by a sedimentation step.

The production phase occurred in serum-free media 48 hours after culture selection by puromycin. The culture medium was replaced twice, first with 50% and after with 75% volume of serum-free media. The final supernatant was collected after 2–3 days and filtered through a 0.2 μm filter, before storage at – 20 ºC for further protein analysis.

2.5.3. Protein analysis

2.5.3.1. SDS-PAGE analysis

Protein samples were separated by sodium dodecylsulphate (SDS) polyacrylamide gel electrophoresis (PAGE) (stacking gel: T = 5%, C = 2.6%, pH 6.8; separating gel: T = 12%, C = 2.6%, pH 8.8) (Sambrook [119]) in SDS-PAGE running

buffer. Before loading onto the gel, protein samples were mixed with protein loading dye containing SDS and β-mercaptoethanol and denatured at 100ºC for 5 minutes.

Samples to be analyzed with immunoblot analysis were submitted the same procedure. Gel dimensions were always 73 mm × 84 mm × 100 mm. The proteins were separated electrophoretically within contant 80 V for 90-120 min. Protein bands were stained with Coomassie brilliant (Pierce®) for SDS-PAGE or transfered to nitrocellulose membrane for immunoblot analysis.

2.5.3.2. Western Blot

Separated proteins were transferred from an SDS-PAGE gel to BIORAD® nitrocellulose membrane (0.45 μm) in transfer buffer, at a constant intensity of 30V overnight.

After blotting the membrane was blocked with 1x PBS buffer containing 5% (w/v) Bovine Serum Albumin (BSA) (milk powder). As primary antibody hLIF 200 μg/ml (rabbit polyclonal Santa Cruz™) was used in a dilution of 1:500 in 1x PBS. Binding of the primary antibody was detected by addition of goat anti-rabbit secondary polyclonal antibody (Santa Cruz™), used in a dilution of 1:1000, coupled to horseradish peroxidase (HRP) enzyme. The target protein was finally revealed by addition of the substrate (Western Blotting Luminol Reagent, Santa Cruz™).

2.5.3.3. ELISA assay

A Quantikine ELISA kit (R&D systems) was used for screening samples for human Leukemia Inhibitory Factor. The protocol and calibration curve was performed as recommended by the kit protocol.

2.6. Data Analysis

For cell growth and aggregate size distribution, results are presented as mean ± standard error of the mean (SEM) of two internal duplicates. For comparing

hLIF secretion in supernatants, internal duplicates were tested in ELISA assay, following further kit's indications.

Origin ® 8 software and Excel 2007 were used in order to reach a more accurate μ_{max} value for growth experiments. The process strategy is described in Appendix, 6.3.

3. Results and Discussion

The optimum temperature and pH value for HEK293 cell culture were previously defined as 37° C and 7.4, respectively [93], in static culture. The agitation rate of 80 rpm for HEK293 cell growth in a 100 mL working volume spinner flask was previously optimized at BERG/IBB-IST.

When in culture, either in static or spinner flask, the cells presented themselves individualized in suspension, as shown in Figure 3.1.

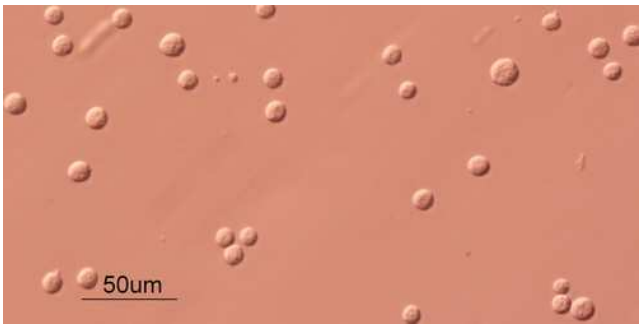

Figure 3.1 – HEK293-EBNA1 cells in suspension at day 0 of culture in a spinner flask.

After seeding, HEK293 cells start as a suspension culture and tend to aggregate if in suspension stirred culture, or to adhere to a surface under static conditions, as a consequence of the need of anchorage for growing. Figure 3.2 shows adherent HEK293-EBNA1 cells on the surface of a T-Flask.

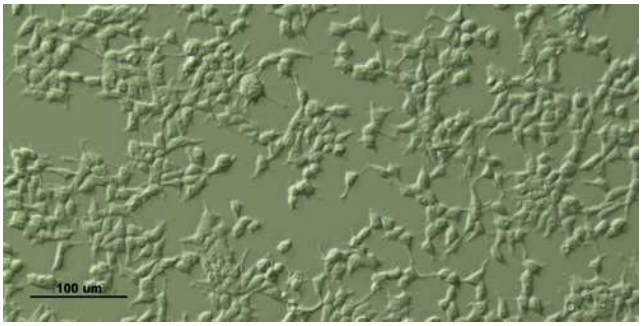

Figure 3.2 – HEK293-EBNA1 cells adherent to a T-flask surface at day 3 of culture.

Optimization of the initial cell density and feeding regime was performed under dynamic conditions in a spinner flask. The results of cell expansion and recombinant hLIF production were then compared with the former method described for T-flask culture.

3.1. Effect of Initial Density on Cell Growth

The effect of inoculation cell density was evaluated in fed-batch experiments of HEK293-EBNA cell growth as described (Materials and Methods, 2.3). Three initial cell densities were tested in spinner flask culture, 2×10^4, 2×10^5 and 2×10^6 cells.mL^{-1}. The feeding regime was setup at 25%, which means a daily renewal of 25 mL (out of 100 mL) of fresh medium. The cellular growth profiles and hLIF production for the suspension stirred culture experiments are presented in Figure 3.3 and Table 3.1.

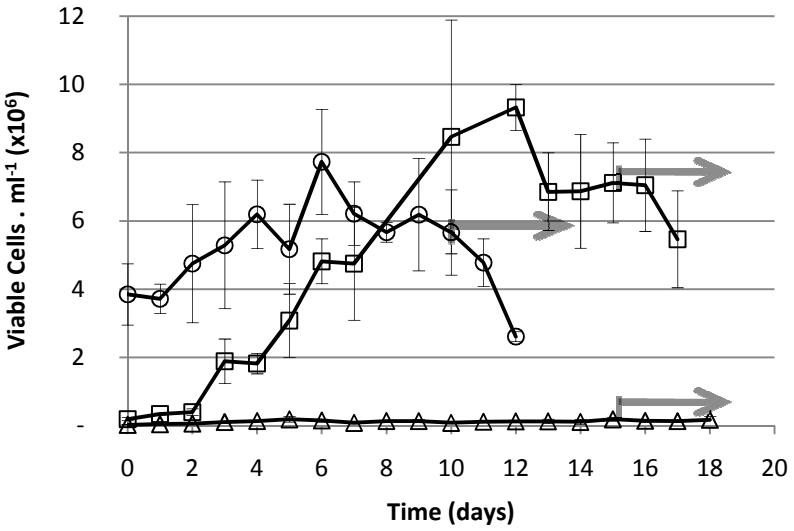

Figure 3.3 – Effect of initial cell density on growth of HEK293-EBNA1 cells. Inocula of 2×10^4 cells.ml^{-1} (△), 2×10^5 cells.ml^{-1} (□), and 2×10^6 cells.ml^{-1} (○) were tested in suspension culture in spinner flask with an agitation rate of 80 rpm and a feeding regime of 25% (v/v) daily medium change. Gray arrows indicate the production of recombinant hLIF in serum-free conditions.

An average cell density of 6.5×10^6 cells.mL^{-1} at production phase start was observed for the inoculum of 2×10^5 cells.mL^{-1} (Figure 3.3). For this condition a maximum fold increase (FI) of 49.6 in total cell number (Table 3.1) was observed and a maximum specific growth rate of 0.055 h^{-1} was attained. For the inocula of 2×10^6 cells.mL^{-1} and 2×10^4 cells.mL^{-1}, lower maximum cell densities were and different growth kinetics were obtained, traduced by specific growth rate values of 0.050 h^{-1} and 0.001 h^{-1}, respectively (Table 3.1). A sampling error should be considered at 2×10^6 cells.ml^{-1} curve once it has double density of inoculum.

Table 3.1 – Maximal growth rates, duplication time and maximal fold increase in total cell number for HEK293-EBNA1 cell growth with a feeding regimen of 25% (v/v) daily.

Initial Cell Density	μ_{max} (h^{-1})	t_d (h)	Fold Increase	X max (10^6 cells.mL^{-1})	X prod (10^6 cells.mL^{-1})
2×10^6 cells.mL^{-1}	0.021	33.0	2.17	7.73	4.35
2×10^5 cells.mL^{-1}	0.055	12.7	49.6	9.32	6.54
2×10^4 cells.mL^{-1}	0.0010	510	29.0	0.188	0.160

Having similar specific growth rates, initial cell densities of 2×10^5 cells.mL^{-1} and 2×10^6 cells.mL^{-1} need different times to achieve the plateau, limiting the F.I. of respective cultures. *Lee et al.* [120] reported and discussed that the specific growth rate of hybridoma cells in a batch suspension culture was found to increase with increasing initial cell density up to a certain cell density level (about 5.4×10^5 cells.mL^{-1}) and then to decrease with further increases in initial cell density, as it was observed within the HEK293-EBNA1 fed-batch suspension culture experiments. Three reasons have been proposed to explain why the specific growth rate increases with increased initial cell density up to a certain level. First, cells can secrete autocrine growth factors (*i.e.* mitogens) that stimulate cell growth during the initial lag phase. Second, cells possess detoxification ability in their environment. Third, there is a specific cell-cell interaction. Nevertheless, further increases in initial cell density result in a reduced specific growth rate. *Lee et al.* [120] also suggests that high maintenance energy and the accumulation of toxic metabolites at high initial cell density reduce specific growth rate.

Moreover, the daily medium change modifies the concentration of autocrine signal factors in the medium [30, 31] and this could affect HEK293-EBNA1 cell expansion. *Chioni et al* [121] reported that FGF-10 acts as a paracrine signalling molecule and seems to play an important role in animal cell proliferation. The concentration of this or equivalent protein in the bulk can be growth inhibitory for the inoculum of 2×10^6 cells.ml^{-1} and not sufficient for cell proliferation for the inoculum of 2×10^4 cells.mL^{-1}.

HEK293-EBNA1 cells showed a strong tendency to form aggregates when cultivated in suspension in serum-containing medium [93]. The HEK293 aggregate size-distribution dynamics is described bellow in Figure 3.4 and Figure 3.5.

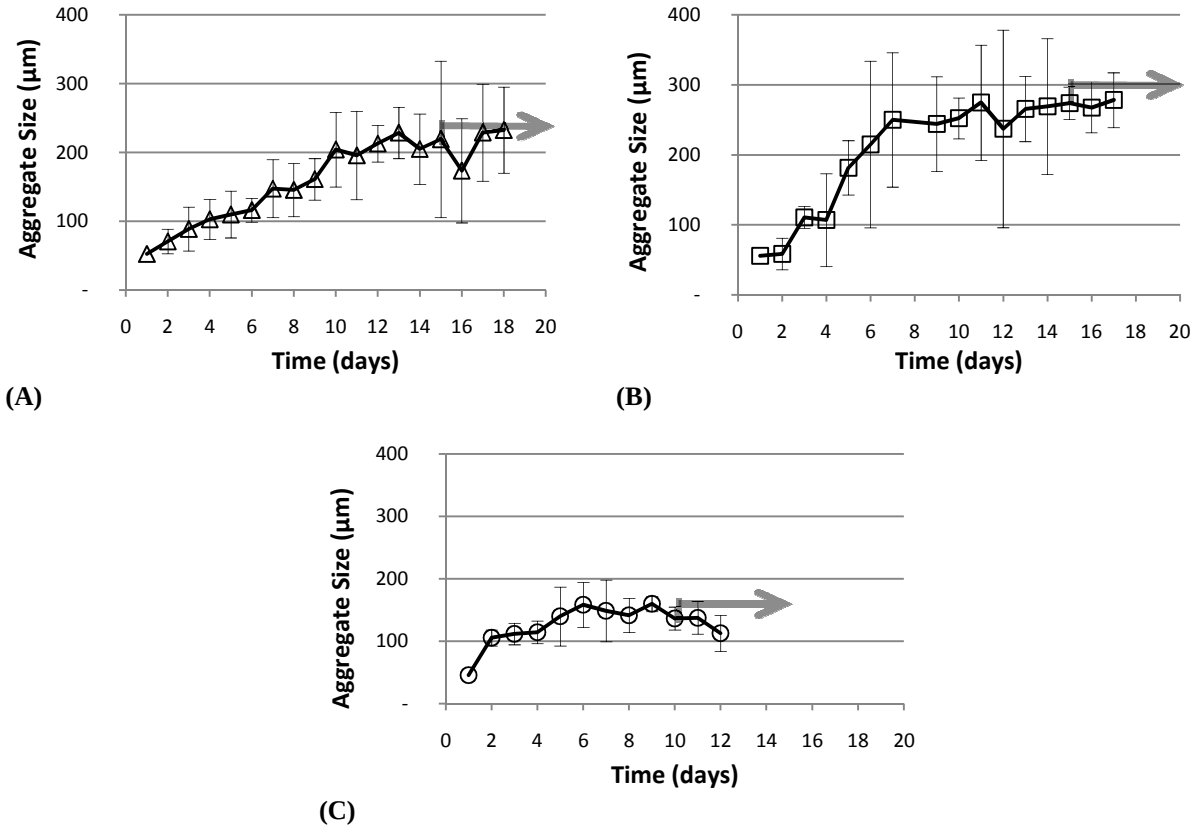

Figure 3.4 – Effect of initial cell density on aggregate size distribution of HEK293-EBNA1 in suspension stirred culture. Inoculums of (A) 2×10^4 cells.mL^{-1} (△); (B) 2×10^5 cells.mL^{-1} (□); (C) 2×10^6 cells.mL^{-1} (○) were tested at an agitation rate of 80 rpm and a feeding regimen of 25% of daily medium change. Gray arrows indicate the production of recombinant hLIF in Serum-Free conditions.

Aggregation of single cells occurred during the first day of culture. Twenty-four hours after the inoculation, spherical HEK293-EBNA1 aggregates with an average diameter around 55 µm were observed in the bulk of all experiments at 80 rpm. The average size of the cellular aggregates increased with culture time, shifting from 53 µm at day 1, to about 233 µm at day 13, for the inoculum of 2×10^4 cells.mL^{-1} (Figure 3.4A), and for the inoculum of 2×10^5 cells.mL^{-1} (Figure 3.4B) the aggregate size distribution started in 56 µm at day 1, increasing to a maximum average of 278 µm at day 11 of culture time. Relatively smaller aggregates were obtained for the inoculum of 2×10^6 cells.ml^{-1} (Figure 3.4C), shifting from 46 µm to 160 µm from day 1 to day 6, respectively. These smaller aggregate sizes could be a consequence of the high initial

cell density once the portion of cells involved in aggregate formation was in great majority.

The standard deviation traduces the heterogeneity of the cellular aggregates, only having some homogeneity in the experiment with higher inoculum (2×10^6 cells.mL^{-1}). The microscopy images of the HEK293-EBNA1 aggregates are shown in Figure 3.5.

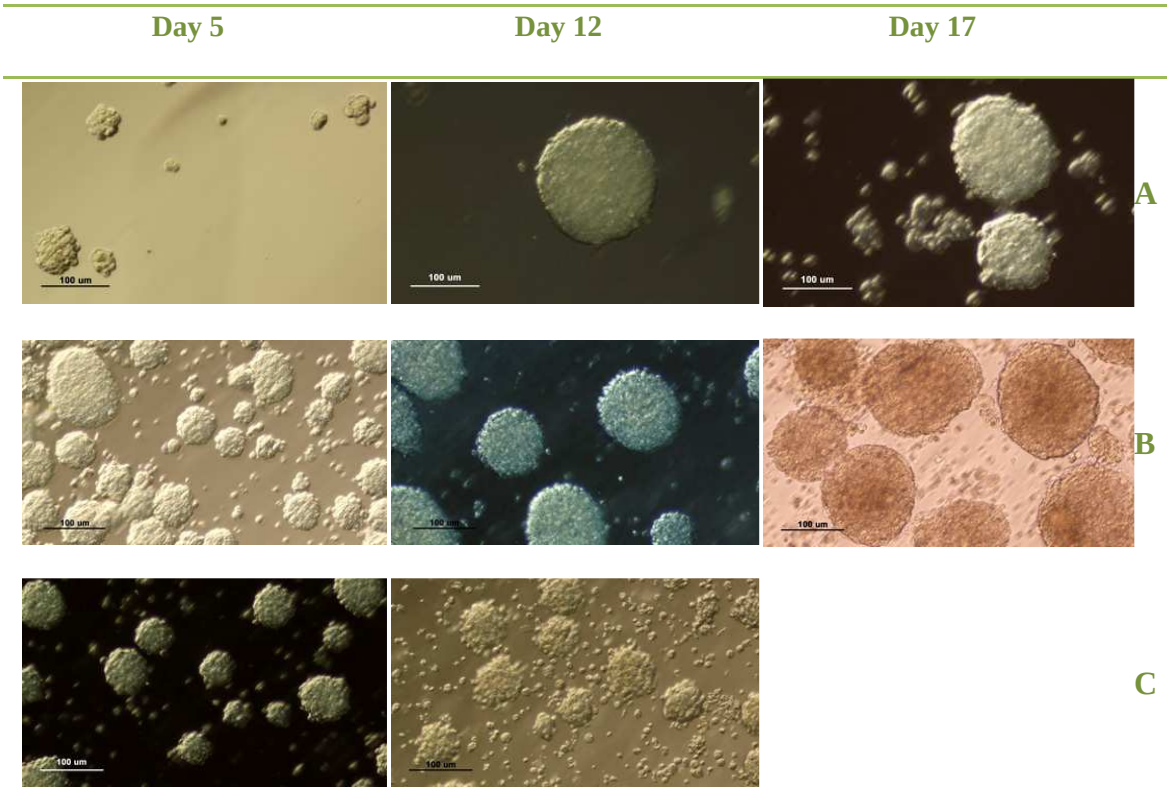

Figure 3.5 – Optical microscopy observations of HEK293-EBNA1 cell aggregates at day 5, 12 and 17 of suspension stirred culture. A – inoculum of 2×10^4 cells.mL^{-1}; B – inoculum of 2×10^5 cells.mL^{-1}; C – inoculum of 2×10^6 cells.mL^{-1} with an agitation rate of 80 rpm and a feeding regimen of 25% of daily medium change. The images at day 17 are in serum-free conditions. Scale bar represents 100 μm length.

At day 5, the number of aggregates directly increases with initial cell density (comparing Figure 3.5A with Figure 3.5C or Figure 3.5B). At day 12, the differences in morphology of aggregates became clear, being smaller with the increase of the initial cell density, and with more cells found as single cells in suspension. At 2×10^4 cells.mL^{-1} inoculum, aggregates kept mostly unchanged from day 12 to day 17 (Figure 3.5A), but slightly larger aggregates occur from day 12 to day 17 (Figure 3.5B) at 2×10^5 cells.mL^{-1}. These images support the data from Figure 3.4.

The inoculum of 2×10^5 cells.mL^{-1} was set as the initial cell density to study the effect of the feeding regimen in HEK293-EBNA1 cell growth and afterwards hLIF production, due to its high cell expansion capacity and more homogeneous aggregate shape and size (presumably not leading to necrosis).

3.2. Effect of Feeding Regimen on HEK293 Cell Growth

Three experiments with the HEK293-EBNA1 cells were setup to study the feeding regimen (FR) of 25%, 50% and 75% daily medium change (Figure 3.6).

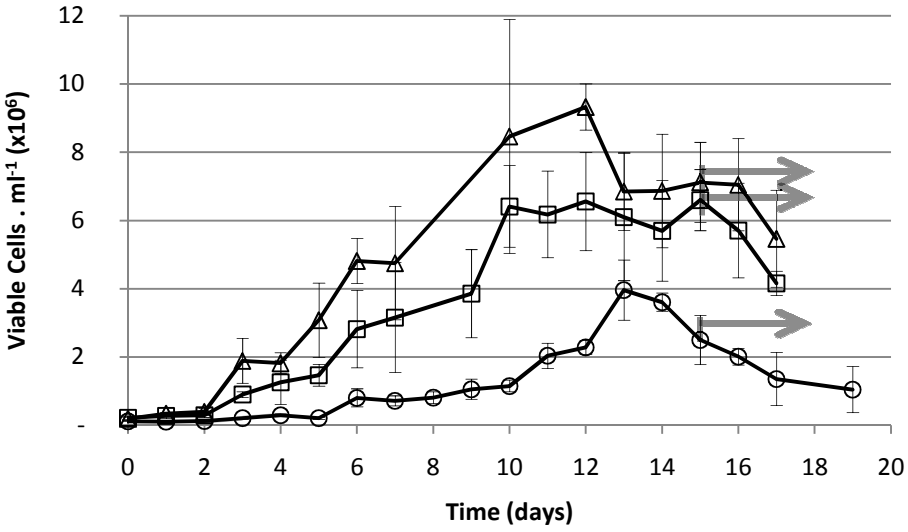

Figure 3.6 – Effect of feeding regime on growth of HEK293-EBNA1 in spinner flask and at 80 rpm
Three feeding regime were tested: 25% (—△—); 50% (—□—); 75% (—○—) of daily medium changes. Gray arrows indicate the production of human LIF in serum-free conditions.

Higher cell densities were observed for the 25% FR. A maximum cell density of 9.3×10^6 cells.mL^{-1} was obtained at day 12 of culture, and an average of 6.54×10^6 cells.mL^{-1} at productions phase in the FR of 25% fresh medium daily renewal, with a FI of 49.6 (Table 3.2). In opposite, lower cell expansion was observed at the FR of 50% and 75%, corresponding to maximal FI in total cell number of 36.8 and 31.6, respectively, and lower cell densities in production phase. The F.I. might be slightly higher than really verified for a FR of 75% due to slightly lower inoculum seeded at day 0, probably caused by a technical issue. As mentioned above in the study of the effect in the initial cell density (Results and Discussion, 3.1), the conservation of secreted autocrine factors provided by a "lower" FR may explain the higher cellular expansion in the FR of 25%. As expected from Figure 3.6 analysis, a higher growth rate was obtained for the FR of 25% (μ_{max} of 0.055 h^{-1}) when compared to the FR of 50% and 75%, μ_{max} of 0.033 h^{-1} and 0.021 h^{-1}, respectively. In Table 3.2, the maximum growth rate,

duplication time, cell densities and FI in total cell number are compared for the FR of 25%, 50%, 75%.

Table 3.2 – Maximal growth rates, duplication time and maximal fold increase in total cell number for a inoculum of 2×10^5 cells.mL^{-1} at different feeding regimen in a spinner flask at 80 rpm.

Feeding Regime	μ_{max} (h^{-1})	t_d (h)	Fold Increase	X max (10^6 cells.mL^{-1})	X prod (10^6 cells.mL^{-1})
25 %	0.055	12.7	49.6	9.32	6.54
50 %	0.033	21.2	31.6	6.60	5.49
75 %	0.021	33.7	36.8	3.96	1.53

The removal and replacement by fresh medium seems to have a negative impact on cell proliferation diminishing the maximum fold increase attained and μ_{max} as the FR increases. The dilution effect caused by fresh medium replacements over proliferative and anti-apoptotic autocrine factors could explain the decrease of the signalling pathways effectiveness activated for cell growth. Thus, this would explain the higher HEK293-EBNA1 cell densities observed for the feeding regime of 25%, with higher maintenance of autocrine factors and lower perturbation on medium composition. Further analysis of metabolites will show how toxic by-products, e.g., lactate and ammonia, may affect culture growth (see Metabolite Analysis, 3.2.1).

The dynamics of HEK293-EBNA1 aggregates during the time of culture was studied (Figure 3.7).

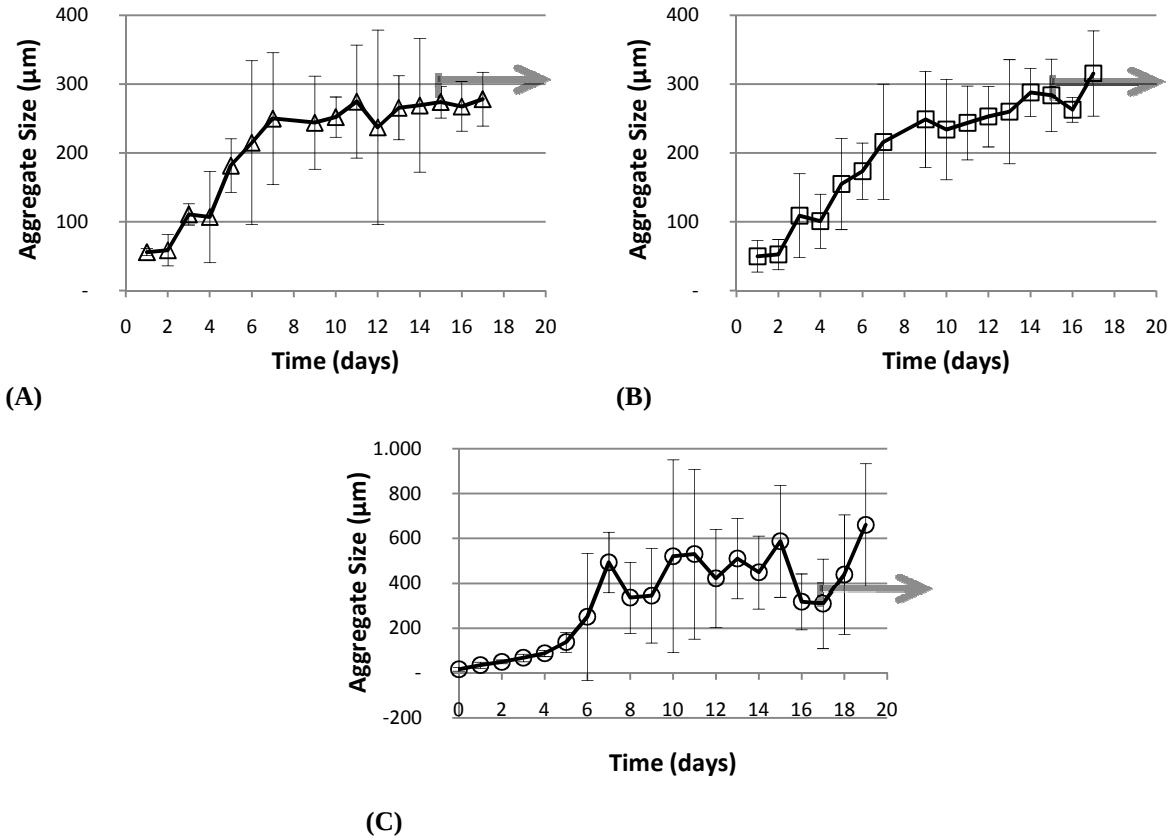

Figure 3.7 – Effect of feeding-regime on HEK293-EBNA1 aggregate size-distribution in suspension stirred culture in spinner flask at 80 rpm The feeding regime of (A) 25% (—△—); (B) 50% (—□—); (C) 75% (—○—) of daily fresh medium renewal are presented. Initial cell density of 2×10^5 cells.mL^{-1}.

The average size of the cell aggregates increased with the time of culture, shifting from 56 µm to 278 µm from day 1 to day 7, for a FR of 25% (Figure 3.7A). Similar results were obtained for the feeding regime of 50%: an increase from 54 µm to 265 µm was observed in the size of HEK293-EBNA1 aggregates from day 1 to day 9 (Figure 3.7B). HEK293 cell aggregates up to 600 µm in diameter were found to have necrotic centres harbouring dead cells [122], what could indicate that high diameter aggregates in 75% F. R. may incur into necrosis (Figure 3.7C).

The microscopy images of the HEK293-EBNA1 aggregates dynamic along culture time are shown in Figure 3.8.

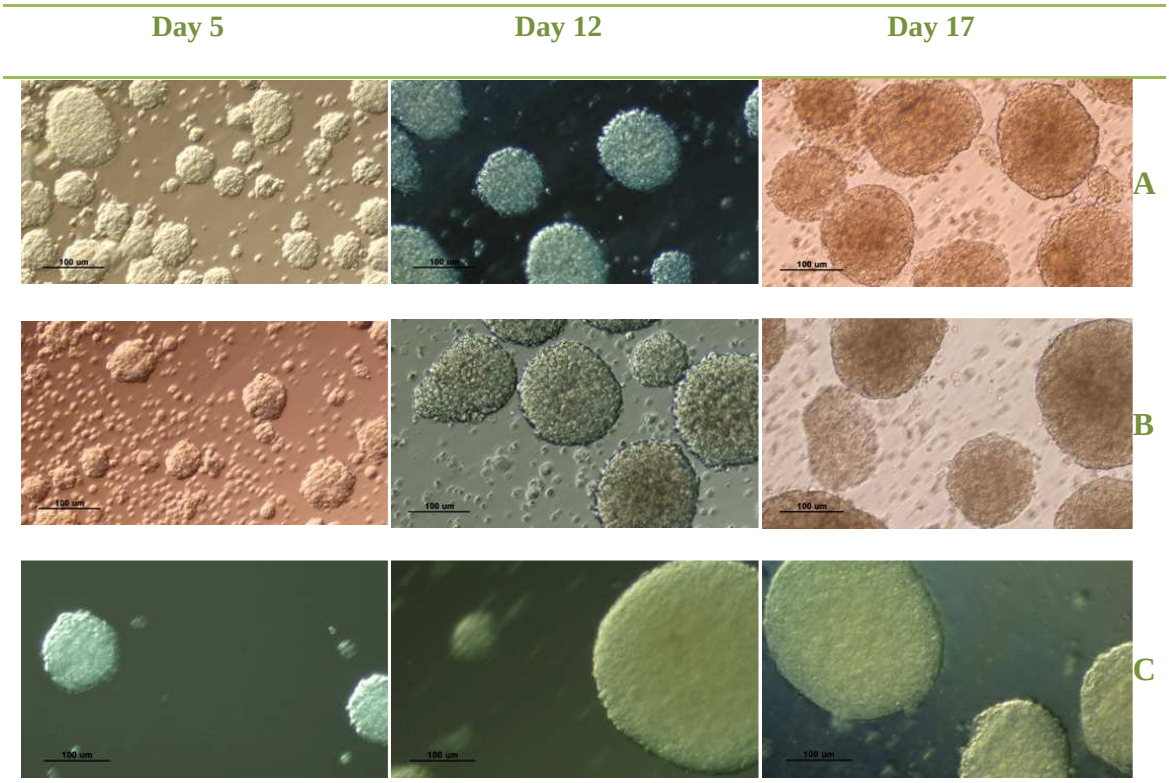

Figure 3.8 – Optical microscopy observations of HEK293-EBNA1 cell aggregates at day 5, 12 and 17 of suspension stirred culture. A – feeding regimen of 25% of daily medium change; B – feeding regimen of 50% of daily medium change; C – feeding regimen of 75% of daily medium change, with an agitation rate of 80 rpm and a start inoculum of 2×10^5 cells.mL^{-1} and with daily medium change. The images at day 17 are in serum-free conditions. Scale bar represents 100 μm

As presented in Figure 3.7, Figure 3.8 shows smaller and homogeneous aggregates observed in the feeding regime of 25% and 50% compared to the heterogeneous aggregates detected with the 75% FR. The data presented seems to predict that considerable volume changes in the suspension culture system of HEK293-EBNA1 cells may have a negative effect in cellular growth leading to aggregate heterogeneity. Thus, the medium renewal, apparently favourable in terms of nutrient replenishment, can provide additional variables that can affect autocrine factors concentration.

Some authors described that aggregates with diameters up to 400 μm have been obtained for BHK and HEK293 cells without having the formation of necrotic centres [123, 124]. *Liu et al* [93] demonstrated that size variation, diffusion limitations, and cell death may exist at the cores of large suspended aggregates. The authors also recommended that the average diameter of aggregates in suspension culture should be controlled to a range smaller than 350 μm, as it was observed in the present work for HEK293-EBNA1 within a feeding regime of 25% and 50% (Figure 3.7A and Figure 3.7B).

3.2.1. Metabolite Analysis

Analysis of the nutrients (glucose and glutamine) consumption and production of catabolites (lactate and ammonia) provides additional information about nutrient limitations once the final cell density could not make it evident. It is important to define the metabolism of the HEK293-EBNA1 cells growing as suspended aggregates in spinner flasks in order to better understand the effect of the feeding regimen on the culture system. Therefore, specific glucose and glutamine consumption rates (q_{glu} and q_{gln}, respectively) as well as specific lactate and ammonia production rates (q_{lac} and q_{amm}, respectively) were determined.

3.2.2. Glucose / Lactate metabolism

Glucose and lactate concentration profiles are presented in Figure 3.9, in order to evaluate the primary metabolism of cells in culture for the different FR at 2×10^5 cells.mL^{-1} initial cell density.

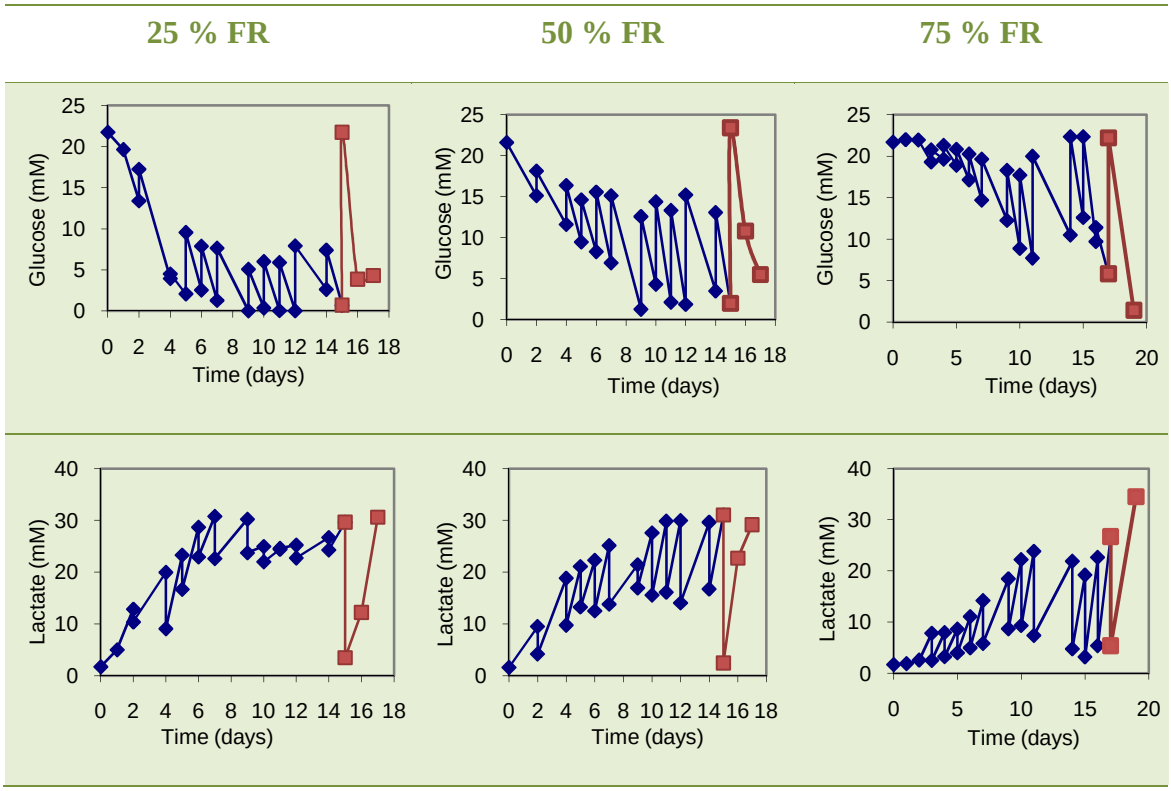

Figure 3.9 – Glucose consumption and Lactate production profiles in suspension stirred culture of HEK293-EBNA1 cell aggregates in spinner flask. The initial cell density was 2×10^5 cells.mL^{-1}. The blue line corresponds to the growth phase in medium supplemented with FBS and the red line corresponds to the production phase under serum-free conditions.

As expected, the feeding regimen affects the availability of glucose in the medium: the higher is the volume of fresh medium renewal, the higher is the glucose concentration available in the medium along time. In the feeding regimen of 25% (Figure 3.9) a significant decrease in glucose concentration was observed after day 3 of cellular growth, probably as a consequence of the higher viable cell density (Figure 3.6), and at day 9 the glucose availability in medium reached zero, keeping this level almost until the end of growth phase. A slightly lower decrease was found for the 50% FR, also with glucose levels near to zero values after day 9. In opposite, the FR of 75% could maintain glucose levels above 5 mM until the last day of culture.

Overall, lactate concentration did not seem to have an inhibitory effect on HEK293-EBNA1 growth. Although *Nadeau et al* [125] referred the 20 mM in lactate as the minimum concentration to have an pronounced effect in cell viability (but not relevant in loss of productivity), *Siegwart et al* [1] registered no limitations on HEK293 growth with lactate concentration until 30 mM. *Newland et al* [126] reported that for tumour cells, the growth was not limited by energy production but rather by biosynthesis rate. *Xie at al* [50] showed that the ATP production per cell was 3-4 times higher than the theoretical ATP needed for biomass and product synthesis and active transport of glucose and amino acids. This over influx of glucose in the cell due to high glucose transport rate, either because the flux of pyruvate in the TCA cycle is limited by a saturated oxidative capacity or because glucose flux directed to the TCA cycle already produces sufficient ATP [127], but this insight cannot be linearly applied to this case, once it will be possible to see that even with glutamine, cell's carbon and energy sources would not be enough as cell's needs, being all available source of energy and carbon applied in growth and protein biosynthesis.

As expectedly, lactate levels, higher in FR of 25% than in 50% and 75% FR are diminished with higher volumes of medium renewals (Figure 3.9). Even tough, all FR could support lactate removal, avoiding concentrations of this by-product above the described inhibitory levels.

3.2.3. Glutamine / ammonia metabolism

Glutamine profiles reveal that availability of this metabolite increase with increase of FR, as described in Figure 3.10. This carbon, nitrogen and energy source clearly complements glucose catabolism in HEK293-EBNA1. If in 50% FR glutamine reached near zero values at day 9 (the same day when occurred glucose starvation), in 25% FR glutamine depletion happens at day 5, four days before glucose depletion. This additional information shows the importance of glutamine as carbon and energy source, simultaneously with glucose. This metabolite is also used as aminoacid or in alanine and proline synthesis, being efficiently recruited for cell growth.

Considering ammonia, for all FR, levels never gone significantly above 4 mM, what might have as consequence futile cycles of NH_4^+ transport, in different extensions upon concentration (that would interfere with electric charges balance) [126].

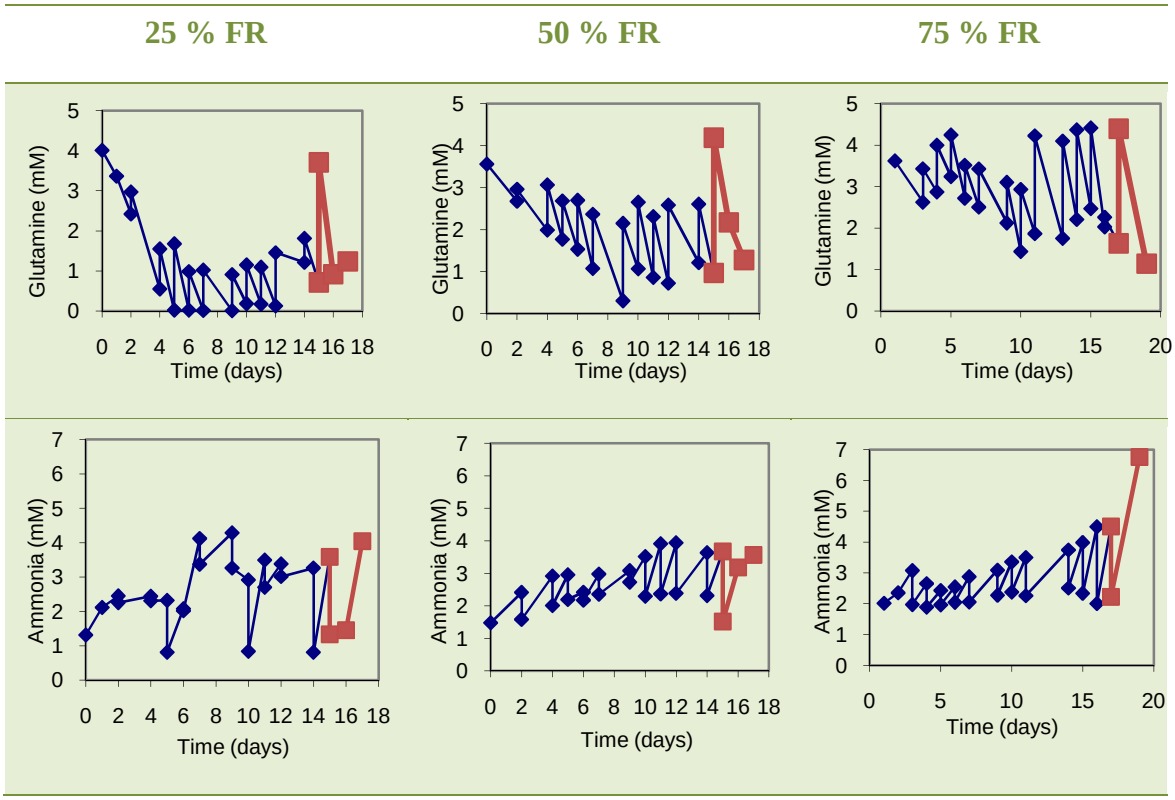

Figure 3.10 – Glutamine and Ammonia production profiles in suspension stirred culture of HEK293-EBNA1 cell aggregates in spinner flask. The initial cell density was 2×10^5 cells.mL^{-1}. The blue line corresponds to the growth phase in media supplemented with FBS and the red line corresponds to the production phase under serum-free conditions.

Figure 3.10 also shows an accumulation of ammonia, being the maximum values reached in the growth phase, 4.29 mM and 3.94 mM for FR of 25% and 50%,

respectively, and in the production phase at 75% FR, with a maximum value of 6.75 mM. For the small difference between ammonia accumulation in 25% and 50% FR, the inhibitory effect on cell growth is not evident and further analysis on this subject would be needed for this confirmation. Furthermore, ammonia tolerance is cell specific and dependent of culture conditions. *Hassel et al.* [49], reported HEK293 as being a resistant cell line to this metabolic stress, at least for 2 mM of external ammonia addition to medium, in comparison to other cell lines. NH_3 easy diffuses across membrane, what favour the accumulation of NH_4^+, competing with potassium for inward transport with the Na^+/K^+, what make ATPase considerably increase maintenance energy.

Borys et al [128] demonstrated that ammonia concentrations on the range of 3-9 mM inhibit the *N*-linked glycosylation in a pH-dependent fashion (in CHO). *Andersen and Goochee* [129] reported similar inhibitory effects were described (also in CHO) on the *O*-linked glycosylation. This occurrence influences directly the biosynthesis and the protein quality. In this study, functional characterization was not performed for produced hLIF, therefore, considerations about this subject will not be possible yet.

3.2.4. Consumption / Production rates and metabolic yields

Glucose maximum specific consumption rates were higher for the 25% and 75% FR corresponding to a fast request from cells for this carbon source at the beginning of exponential growth phase but generally lower at production phase, except for the FR of 75% (Table 3.3). This correlates with the high lactate production rates for all FR at growth phase, specially for 75% FR, and lower at the phase of recombinant protein production. According to the high specific consumption glucose rates verified at FR of 75%, this also exhibits the higher values for lactate production.

With this data, a direct relation about glucose consumption or lactate production and cell expansion capacity across different FR could not be found.

Although, considering also the literature relation of high glucose/ high lactate levels, a decrease in glucose feeding could eventually be tested in order to find a metabolic shift.

Table 3.3 – Metabolic specific consumption (glucose, glutamine) and production (lactate, ammonia) rates. Maximum values were obtained to characterize growth exponential phase and average values were obtained to characterize cell culture afterwards (after day7) including production phase (the presented units are in μmol.10^6 cells.day^{-1})

FR	q Glu $_{max}$	$\overline{q\ \mathbf{Glu}}$	q Lac $_{max}$	$\overline{q\ \mathbf{Lac}}$	q Gln $_{max}$	$\overline{q\ \mathbf{Gln}}$	q Amm $_{max}$	$\overline{q\ \mathbf{Amm}}$
25%	32.8	2.16	41.2	1.16	4.96	0.309	0.921	0.342
50%	9.83	3.31	16.1	3.69	1.84	0.494	1.64	0.359
75%	32.1	10.0	54.4	17.9	7.66	1.52	7.31	1.85

The 25% and 75% FR displayed the higher glucose and glutamine specific maximum consumption rates (Table 3.3), revealing high needs in this nutrients at exponential growth. These rates significantly decrease after growth phase in all FR, being the 75% FR who kept the higher consumptions along the further time of culture.

Ammonia production rates were generally higher for exponential growth than later, on all FR. Particularly; in the 75% FR, a relatively high maximum at growth phase was found, corresponding also to a high value of glutamine consumption at exponential growth. This can be an immediate consequence of glutamine double deamidation (second ammonia molecule removal), mechanism not so evident for 25% FR witch glutamine consumption did not had such a significant impact in ammonia production. In this case, a redirection of glutamine into the aminoacid metabolism could occurred, once in 25% FR high culture expansion might had request this glutamine for biosynthesis.

Maximum lactate from glucose yield ($Y'_{lac/glu}$ *max*) was obtained from exponential growth phase (until day 7 of culture) and average lactate from glucose yield ($\overline{Y'}_{lac/glu}$) was calculated from daily values average (since day 7) for further culture time, respectively for each FR (Table 3.4).

Table 3.4 – Apparent yields of suspension stirred culture of HEK293-EBNA1 cell aggregates in spinner flask. Apparent yield of lactate from glucose as a function of culture time is represented.

	25 % FR	50 % FR	75 % FR
$Y'_{\frac{lac}{glu}(max)}$	3.12	4.20	4.96
$\overline{Y'}_{\frac{lac}{glu}}$	0.628	1.21	1.79

Maximum $Y'_{lac/glu}$ were relatively high in all FR, showing an intense request of carbon and energy directly from glycolysis, through fermentation, with consequent lactate formation. This yield increases upon FR volume increase what might reveal a lower metabolic efficiency in higher FR.

Average $Y'_{lac/glu}$ values are generally lower than maximum $Y'_{lac/glu}$ as a consequence of a lower energetic request for cellular proliferation mechanisms after exponential growth. This yield also has a direct increase with FR, suggesting that in 25% FR cells could have a more successful management of metabolic resources since it resulted in higher cell expansion with best use of carbon, and lower by-products (like lactate) biosynthesis.

Average values above 2, that is the theoretical limit since one mole of glucose yields 2 moles of lactate, generally reveal that glycolysis is used as a fast pathway for energetic metabolism. However, no information about oxygen uptake could support further discussion about the extension of anaerobic or aerobic respiration along culture time.

Offline measures of metabolic yields are difficult to achieve good consistency, once that kinetics could be not synchronized, and therefore these ratios miss estimated.

The effect of the feeding regime on growth and aggregate size distribution was also evaluated for the initial cell density of 2×10^6 cells.mL^{-1}, but no metabolic analysis was performed. This data is presented in Appendix, 6.4.

3.3. Effect of the global culture strategy on cell growth

In Table 3.5 the data obtained in the present work is compared to different animal cell culture strategies described in the literature, namely for static or dynamic systems.

Table 3.5 – Comparison of culture strategies for growth of HEK293 cells. (The results of the present work were obtained in static conditions for monolayer culture, and in suspension stirred conditions at spinner flask to compare with fed-batch culture).

	monolayer		batch	fed-batch	*spinner flask*	perfusion
	Liu et al [93]	*present work*	*Siegwart et al* [1]	*Liu et al* [93]	*present work*	*Siegwart et al* [1]
μ_{max} (h^{-1})	0.041±0.02	0.022	0.022	0.037±0.07	0.033	0.034
Maximum Viable Cell Density (10^6 cells.mL^{-1})	2.41±0.37	1.45	1	5.24±0.51	6.56	1
q_{glu} (µmol/10^6 cells.h^{-1})	9.3±0.6	-	0.33	8.5±0.4	3.31	0.10
q_{lac} (µmol/10^6 cells.h^{-1})	14.7±1.6	-	0.67	14.3±1.2	3.69	0.17
$Y'_{lac/glu}$ (mol.mol^{-1})	1.58	-	2.00	1.68	1.21	1.6

The comparison of data obtained can bring new insights about HEK293 growth and animal cell metabolism. In the monolayer culture, performed in T-flask, *Liu et al* [93], reported a higher growth rate and maximum cell density when compared to the data obtained in the present work, 0.041 h^{-1} and 2.41×10^6 cells.mL^{-1} *vs* 0.022 h^{-1} and 1.45×10^6 cells.mL^{-1}, respectively. This could be due the fact that different media were used in the experiments: DMEM medium was used in the present work and Ham's F-12, mixed with DMEM medium, was used by *Liu et al.* [93], where cells were passaged every 4–5 days at a seeding density of $1–2\times10^5$ cells mL^{-1}.

Table 3.5 also shows that in our 50% FR suspension stirred culture (2×10^6 cells.mL^{-1} inoculum, 80 rpm) and in *Liu's* fed-batch the HEK293 cells almost grown with same maximum growth rate, reaching closer maximum viable cell densities. Slower average glucose consumption and lactate production rates were registered in our

study, but in this case, our experiments verified a constant feeding regime whereas *Liu's et al* [93] HEK293 fed-batch used an increasing feeding-regime from 30% to 90%, which directly affects variable medium removal of lactate and differential glucose availability.

Siegwart et al [1] performed a fed-batch culture with a perfusion system in a low calcium serum-free medium (LC-SFM) in a online controlled process with glucose concentration maintained at 1 mM. This system has the capacity of keeping a μ_{max} of 0.034 h^{-1} with very low glucose consumption rate and low lactate production rate, having obtained a maximum cell viability of 1×10^{6} cells.mL^{-1}, what would give a good support for protein production in relatively controlled conditions (still to confirm).

Either *Siegwart et al* [1] batch or perfusion methods seem to achieve low q_{glu} and low q_{lac}, rationalizing use of glucose and inhibition by lactose, but in terms of cell expansion this strategies would not represent an option. The reduced influx of 1 mM glucose, in perfusion, could help to maintain the HEK293 cell culture without significant kinetic's change, but avoiding excess of glucose to enter in secondary metabolic fluxes directed to lactate production. As it was mentioned before (Results and Discussion, 3.2.2), this could be helpful in order to avoid inhibitory concentrations of lactate in the medium and thus, preventing acidification and a more rational use of the available glucose for primary metabolism.

It should be noticed that Siegwart's experiments were performed at serum-free conditions

Considering the different results obtained for different experimental conditions, culture parameters could still be modified to enhance cell growth. Media, culture system and feeding regime are the main variables to optimize in order to bring higher cell productivities, and turn this system robust for industrial applications.

3.4. Recombinant Human Leukemia Inhibitory Factor (hLIF) Quantification and Productivity Analysis

The hLIF production phase starts after the puromycin selection in the stationary phase of HEK293-EBNA1 cell culture and in serum-free conditions. This strategy will provide supernatants enriched in hLIF and free of contaminant proteins derived from serum, which will also significantly facilitate the subsequent recovery and purification process (downstream process). In order to confirm the expression of hLIF, sodium dodecyl-sulfate polyacrylamide gel electrophoresis (SDS-PAGE) and Western Blot analysis of supernatants were performed (

Figure 3.11).

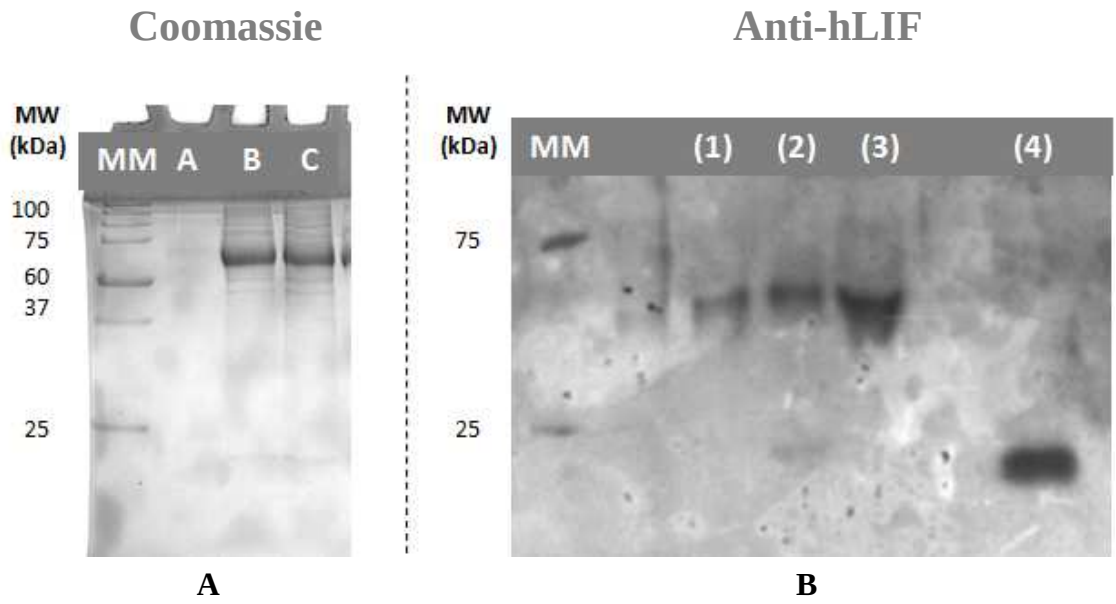

Figure 3.11 – SDS-PAGE (A) and Western Blot (B) Analysis of the supernatants obtained at the end of the production phase of hLIF in serum-free conditions. *Lane A*: monolayer static culture, *Lane B*: spinner flask suspension culture with FR of 25% at 80 rpm, *Lane C*: spinner flask suspension culture with FR of 50%.at 80 rpm. *Lane 1*: monolayer static culture, *Lane 2 and 3*: spinner flask suspension culture with FR 50% and at 80 rpm, *Lane 4*: hLIF standard (Chemicon®). *Lane MM*: molecular markers.

In

Figure 3.11A, a protein band around 70kDa was observed pointing to expression of recombinant hLIF. Production in spinner flasks leads to more intense protein band around 70kDa than monolayer cultures. This was confirmed by Western-Blot analysis

where a stronger hLIF band was observed for the spinner flask cultures when compared to monolayer (

Figure 3.11B). Intensity differences from Lane 2 and 3 may due the different load of samples on gel. The reference of hLIF displays a band around 20 kDa in the Western-Blot, which corresponds to the predicted molecular weight for the non glycosilated form. The Western Blot also revealed a band at 70 kDa, either in static or in spinner flask cultures, what may suggest the presence of hLIF as a dimmer.

Enzyme Linked Immuno-Sorbent Assay (ELISA) allowed the quantification of hLIF and the calculation of specific productivities for the production of recombinant hLIF in animal cell culture (HEK293). For spinner flask experiments, specific productivities were calculated with basis on average viable cell density at the production phase, under serum-free conditions; in static culture, final cell density was used instead. Table 3.6 presents an overall view of the present work with the additional information of hLIF concentration in the bulk and specific productivities.

Table 3.6 – Production of recombinant hLIF using HEK293-EBNA1 cells in different culture systems. Growth parameters and productivities are presented.

Culture system	Inoculum (cells.mL^{-1})	Feeding Regime (day^{-1})	FI $_{Max}$	Agg. Size $_{max}$ (µm)	μ_{max} (h^{-1})	hLIF (ng.mL^{-1})	SpecifichLIF Production (ng.10^6 cell^{-1})
Spinner flask	**2×10^4**	25 %	29 ± 19.7	233	0.0014	-	-
	2×10^5	25 %	50 ± 10.7	278	0.055	125 ± 2.2	19.1
		50 %	32 ± 9.2	315	0.033	90.0 ± 5.72	16.4
		75 %	37 ± 9.6	660	0.021	48.1 ± 4.21	31.4
	2×10^6	25 %	2.6 ± 1.66	160	0.021	93.1 ± 7.20	21.4
Monolayer	**2×10^5**	-	7.3	-	0.022	40.0 ± 1.21	37.9

Of all the tested conditions and culture systems, the spinner flask culture with an initial cell density of 2×10^5 cells.mL^{-1} and a feeding regimen of 25% daily medium change was the experiment that lead to a higher recombinant hLIF volumetric productivity (125±2.2 ng.mL^{-1}). A decrease in the volumetric productivity with the increase of the FR volume was observed, although the specific productivity is quite similar for the feeding regime of 25% (both 2×10^5 cells.mL^{-1} and 2×10^6 cells.mL^{-1}

inoculums) and 50% (at 2×10^5 cells.mL^{-1} inoculum), representative of the importance of high number of viable cell maintenance in culture.

The value of 75% FR with a 2×10^5 cells.mL^{-1} inoculum for specific productivity is similar to the obtained for the monolayer culture, 31.4 ng.10^6 cell^{-1} and 37.9 ng.10^6 cell^{-1}, respectively. However, since ratio of available surface area in monolayer culture is low, the volumetric productivity decreases to 40.0±1.2 ng.mL^{-1}. High specific productivity of 75% FR at 2×10^5 cells.mL^{-1} reflects not a good cell capacity but the low maintenance of viable cells at end of culture, considereing the lower volumetric productivity, 48.1 ± 4.21 ng.10^6 cell^{-1} when compared with other FR for same inoculum.

4. Conclusions and Future Trends

Human Leukemia Inhibitory Factor was successfully expressed in the previously established HEK293-EBNA1 cells. The effects of the different initial cell densities and feeding regime were studied towards the maximization of the recombinant protein productivities.

4.1. Conclusions

The inoculum 2×10^5 cell.ml^{-1} at 25% of daily medium change allowed to reach a higher number of total viable cells, 7×10^6 cells.mL^{-1} with a μ_{max} of 0.055 h^{-1}. At these conditions, HEK293-EBNA1 aggregates at production phase reached a maximum diameter of 270 μm. When comparing this feeding regime with 50% and 75% a gradual decrease on maximum cell number and maximum growth rate was observed.

Metabolite analysis was performed for 25%, 50% and 75% of daily medium change experiments with an initial cell density of 2×10^5 cell.ml^{-1}. Glucose and glutamine were found to be complementary carbon and energy sources for cell metabolism. Lactate was produced as a consequence of the high glycolysis rate but not in severe inhibitory concentrations. Although the ammonia levels were relatively high, it did not seem to have an evident inhibitory role for HEK293-EBNA1 culture due to its relative tolerance to this metabolite (further tests would be recommended).

All the dynamic culture systems demonstrated to be able to produce higher volumetric productivities of hLIF rather than in monolayer culture, being the 25% feeding regime at an initial cell density of 2×10^5 cell.ml^{-1} the experiment with the higher value, 125 ± 2.20 ng.mL^{-1}. For this inoculum both 25 and 50% feeding regime showed similar specific hLIF productivities, 19.1 and 16.4 ng hLIF.10^6 cell^{-1}.

4.2. Future trends

Spinner flask experiments are useful to study parameters such as inoculum densities, feeding regime strategies, agitation rate, by-products inhibition and others. However, small scale, fully controlled bioreactors (1 L) are still needed for comprehension of complex biological systems for large scale expression systems. In these, the respiration rate (q_{O2}), mass and heat transfer, shear stress and foam formation are other variables to undergo other level of biopharmaceutical engineering.

Nevertheless, more studies could help to validate the proficiency of the parameters established for spinner flask culture and the quality of recombinant hLIF produced:

- Test the autocrine factors involved in cell proliferation. ELISA or Western Blot procedures could be tried for factors like VEGF, HGF or FGF2 as suggested by *Weil* [130].
- **Quality control of produced hLIF:** (1) by addressing his capacity on 46C mouse embryonic stem cell pluripotency maintenance; (2) through biological quantification of specific activity in M1 cell line (standard test).
- **Scale-up:** start a bioreactor with the previous knowledge obtained with the spinner flask experiments (seeding inoculum of 2×10^5 cell.ml^{-1}; feeding regime of 25% daily medium change)
- **New Feeding Regime strategies:** (1) use medium change every 12h with half of volumes tested before to avoid large variations on nutrient availability, as well as autocrine factors; (2) establish a culture feeding system by perfusion; and (3) test new reactor designs (ex: Wave® Bioreactor) .
- **Downstream Process:** test protocols for purification and clarification of the target product that is hLIF, being ion exchange chromatography one of the preferably strategies for this issue.

5. References

1. Siegwart, P.; Cote, J.; Male, K.; Luong, J. H. T.; Perrier, M.; Kamen, A., Adaptive control at low glucose concentration of HEK-293 cell serum-free cultures. *Biotechnology Progress* 1999, 15, (4), 608-616.
2. Wurm, F. M.; Matasci, M.; Hacker, D. L.; Baldi, L., Recombinant therapeutic protein production in cultivated mammalian cells: current status and future prospects *Drug Discovery Today: Technologies* 2009, Article in Press.
3. Langer, L. J., U.S. bitech symposium focuses on bioprocessing: economic strategies to increase production yelds. *Gen Eng News* 1999, 19, (1), 1-14.
4. Griffin, T. J.; Seth, G.; Xie, H.; Bandhakavi, S.; Hu, W. S., Advancing mammalian cell culture engineering using genome-scale technologies. *Trends Biotechnol* 2007, 25, (9), 401-8.
5. Wurm, F. M., Production of recombinant protein therapeutics in cultivated mammalian cells. *Nat Biotechnol* 2004, 22, (11), 1393-8.
6. Delehedde, M.; Sarrazin, S.; Adam, E.; Motte, V.; Vanpouille, C., Proteoglycans and glycosaminoglycans: complex molecules with modulating activity. *New Developments in Therapeutic Glycomics* 2006, Research Signpost, (Kerala), 1-13.
7. Ohtsubo, K.; Marth, J. D., Glycosylation in cellular mechanisms of health and disease. *Cell* 2006, 126, (5), 855-67.
8. Jelkmann, W., Erythropoietin after a century of research: younger than ever. *Eur J Haematol* 2007, 78, (3), 183-205.
9. Ho, R. J. Y.; Gibaldi, M., *Biotechnology and Biopharmaceuticals: Transforming Proteins and Genes into Drugs*. WileyBlackwell: 2003; p 576.
10. McCafferty, J.; Glover, D. R., Engineering therapeutic proteins. *Curr Opin Struct Biol* 2000, 10, (4), 417-20.
11. Qiu, J., Protein expression systems. *Gen Eng News* 1998, 18, 17-40.
12. Demain, A. L.; Vaishnav, P., Production of recombinant proteins by microbes and higher organisms. *Biotechnol Adv* 2009, 27, (3), 297-306.
13. Elbein, A. D.; Mitchell, M.; Molyneux, R. J., Effect of castanospermine on the structure and secretion of glycoprotein enzymes in Aspergillus fumigatus. *J Bacteriol* 1984, 160, (1), 67-75.
14. Nunberg, J. H.; Meade, J. H.; Cole, G.; Lawyer, F. C.; McCabe, P.; Schweickart, V.; Tal, R.; Wittman, V. P.; Flatgaard, J. E.; Innis, M. A., Molecular cloning and characterization of the glucoamylase gene of Aspergillus awamori. *Mol Cell Biol* 1984, 4, (11), 2306-15.
15. Jenkins, N.; Curling, E. M., Glycosylation of recombinant proteins: problems and prospects. *Enzyme Microb Technol* 1994, 16, (5), 354-64.
16. Goldwasser, E.; Kung, C. K.; Eliason, J., On the mechanism of erythropoietin-induced differentiation. 13. The role of sialic acid in erythropoietin action. *J Biol Chem* 1974, 249, (13), 4202-6.
17. Wittwer, A. J.; Howard, S. C., Glycosylation at Asn-184 inhibits the conversion of single-chain to two-chain tissue-type plasminogen activator by plasmin. *Biochemistry* 1990, 29, (17), 4175-80.
18. Cantell, K.; Hirvonen, S.; Sareneva, T.; Pirhonen, J.; Julkunen, I., Differential inactivation of interferons by a protease from human granulocytes. *J Interferon Res* 1992, 12, (3), 177-83.
19. Yamaguchi, K.; Akai, K.; Kawanishi, G.; Ueda, M.; Masuda, S.; Sasaki, R., Effects of site-directed removal of N-glycosylation sites in human erythropoietin on its production and biological properties. *J Biol Chem* 1991, 266, (30), 20434-9.
20. Datar, R. V.; Cartwright, T.; Rosen, C. G., Process economics of animal cell and bacterial fermentations: a case study analysis of tissue plasminogen activator. *Biotechnology (N Y)* 1993, 11, (3), 349-57.
21. Aldridge, S., Downstream processing needs a boost. *Gen Eng News* 2006, 26, (1).
22. Zhang, J.; Robinson, D.; Salmon, P., A novel function for selenium in biological system: selenite as a highly effective iron carrier for Chinese hamster ovary cell growth and monoclonal antibody production. *Biotechnol Bioeng* 2006, 95, (6), 1188-97.

23. Ryll, T. In *Antibody production using mammalian cell culture - how high can we push productivity?*, *Abstr.* , , , *Aug (*SIM Ann Mtg Prog and Abstr, San Diego, CA, 2008; San Diego, CA, 2008; p 101.
24. Coco-Martin, J. M.; Harmsen, M. M., A review of therapeutic protein expression by mammalian cells. *BioProcess Int.* 2008, June supplement 28–33.
25. Jarvis, L. M., A technology bet. DSM's pharma product unit leverages its biotech strength to survive in a tough environment. *Chem Eng News* 2008, 86, (8), 30–31.
26. al-Rubeai, M.; Singh, R. P., Apoptosis in cell culture. *Curr Opin Biotechnol* 1998, 9, (2), 152-6.
27. Zeng, A. P.; Deckwer, W. D.; Hu, W. S., Determinants and rate laws of growth and death of hybridoma cells in continuous culture. *Biotechnol Bioeng* 1998, 57, (6), 642-54.
28. Zeng, A. P.; Deckwer, W. D., Model simulation and analysis of perfusion culture of mammalian cells at high cell density. *Biotechnol Prog* 1999, 15, (3), 373-82.
29. Mohan, C.; Kim, Y. G.; Koo, J.; Lee, G. M., Assessment of cell engineering strategies for improved therapeutic protein production in CHO cells. *Biotechnol J* 2008, 3, (5), 624-30.
30. Raff, M. C., Social controls on cell survival and cell death. *Nature* 1992, 356, (6368), 397-400.
31. Raff, M. C.; Barres, B. A.; Burne, J. F.; Coles, H. S.; Ishizaki, Y.; Jacobson, M. D., Programmed cell death and the control of cell survival. *Philos Trans R Soc Lond B Biol Sci* 1994, 345, (1313), 265-8.
32. Anitua, E.; Andia, I.; Sanchez, M.; Azofra, J.; del Mar Zalduendo, M.; de la Fuente, M.; Nurden, P.; Nurden, A. T., Autologous preparations rich in growth factors promote proliferation and induce VEGF and HGF production by human tendon cells in culture. *J Orthop Res* 2005, 23, (2), 281-6.
33. Brieger, J.; Wierzbicka, M.; Sokolov, M.; Roth, Y.; Szyfter, W.; Mann, W. J., Vessel density, proliferation, and immunolocalization of vascular endothelial growth factor in juvenile nasopharyngeal angiofibromas. *Arch Otolaryngol Head Neck Surg* 2004, 130, (6), 727-31.
34. Augustin-Voss, H. G.; Voss, A. K.; Pauli, B. U., Senescence of aortic endothelial cells in culture: effects of basic fibroblast growth factor expression on cell phenotype, migration, and proliferation. *J Cell Physiol* 1993, 157, (2), 279-88.
35. Fuentes, M. A.; Opperman, L. A.; Bellinger, L. L.; Carlson, D. S.; Hinton, R. J., Regulation of cell proliferation in rat mandibular condylar cartilage in explant culture by insulin-like growth factor-1 and fibroblast growth factor-2. *Arch Oral Biol* 2002, 47, (9), 643-54.
36. Hebert, T. L.; Wu, X.; Yu, G.; Goh, B. C.; Halvorsen, Y. D.; Wang, Z.; Moro, C.; Gimble, J. M., Culture effects of epidermal growth factor (EGF) and basic fibroblast growth factor (bFGF) on cryopreserved human adipose-derived stromal/stem cell proliferation and adipogenesis. *J Tissue Eng Regen Med* 2009.
37. Zanghi, J. A.; Fussenegger, M.; Bailey, J. E., Serum protects protein-free competent Chinese hamster ovary cells against apoptosis induced by nutrient deprivation in batch culture. *Biotechnol Bioeng* 1999, 64, (1), 108-19.
38. Iyer, P.; Ostrove, J. M.; Vacante, D., Comparison of manufacturing techniques for adenovirus production. *Cytotechnology* 1999, 30, (1-3), 169-72.
39. Masters, J. R. W., *Animal Cell Culture: A Practical Approach*. 3rd Edition ed.; Oxford University Press, USA: 2000; p 315.
40. Shuler, M. L.; Kargi, F., *Bioprocess Engineering : Basic Concepts*. 2nd Edition ed.; Prentice Hall: 2002.
41. Butler, M., Growth limitations in microcarrier cultures. *Adv Biochem Eng Biotechnol* 1987, 34, 57-84.
42. da Silva, C. L.; Ferreira, B. S.; Cabral, J. M. S., *Bioreactores para cultura de células animais*. Lidel, Edições Técnicas, Lda: 2006; Vol. 1.
43. Schneider, M.; Marison, I. W.; von Stockar, U., The importance of ammonia in mammalian cell culture. *J Biotechnol* 1996, 46, (3), 161-85.
44. Cruz, H. J.; Moreira, J. L.; Carrondo, M. J., Metabolic shifts by nutrient manipulation in continuous cultures of BHK cells. *Biotechnol Bioeng* 1999, 66, (2), 104-13.

45. Fitzpatrick, L.; Jenkins, H. A.; Butler, M., Glucose and glutamine metabolism of a murine B-lymphocyte hybridoma grown in batch culture. *Appl Biochem Biotechnol* 1993, 43, (2), 93-116.
46. Glacken, M. W., Catabolic Control of Mammalian-Cell Culture. *Bio-Technology* 1988, 6, (9), 1041-&.
47. Reitzer, L. J.; Wice, B. M.; Kennell, D., Evidence that glutamine, not sugar, is the major energy source for cultured HeLa cells. *J Biol Chem* 1979, 254, (8), 2669-76.
48. Zielke, H. R.; Zielke, C. L.; Ozand, P. T., Glutamine: a major energy source for cultured mammalian cells. *Fed Proc* 1984, 43, (1), 121-5.
49. Hassell, T.; Gleave, S.; Butler, M., Growth inhibition in animal cell culture. The effect of lactate and ammonia. *Appl Biochem Biotechnol* 1991, 30, (1), 29-41.
50. Xie, L.; Wang, D. I., Material balance studies on animal cell metabolism using a stoichiometrically based reaction network. *Biotechnol Bioeng* 1996, 52, (5), 579-90.
51. Kim, S. H.; Lee, G. M., Down-regulation of lactate dehydrogenase-A by siRNAs for reduced lactic acid formation of Chinese hamster ovary cells producing thrombopoietin. *Appl Microbiol Biotechnol* 2007, 74, (1), 152-9.
52. Park, H.; Kim, I. H.; Kim, I. Y.; Kim, K. H.; Kim, H. J., Expression of carbamoyl phosphate synthetase I and ornithine transcarbamoylase genes in Chinese hamster ovary dhfr-cells decreases accumulation of ammonium ion in culture media. *J Biotechnol* 2000, 81, (2-3), 129-40.
53. Kim, S. H.; Lee, G. M., Functional expression of human pyruvate carboxylase for reduced lactic acid formation of Chinese hamster ovary cells (DG44). *Appl Microbiol Biotechnol* 2007, 76, (3), 659-65.
54. Durocher, Y.; Perret, S.; Kamen, A., High-level and high-throughput recombinant protein production by transient transfection of suspension-growing human 293-EBNA1 cells. *Nucleic Acids Res* 2002, 30, (2), E9.
55. Meissner, P.; Pick, H.; Kulangara, A.; Chatellard, P.; Friedrich, K.; Wurm, F. M., Transient gene expression: recombinant protein production with suspension-adapted HEK293-EBNA cells. *Biotechnol Bioeng* 2001, 75, (2), 197-203.
56. Pham, P. L.; Perret, S.; Cass, B.; Carpentier, E.; St-Laurent, G.; Bisson, L.; Kamen, A.; Durocher, Y., Transient gene expression in HEK293 cells: peptone addition posttransfection improves recombinant protein synthesis. *Biotechnol Bioeng* 2005, 90, (3), 332-44.
57. Blasey, H. D.; Aubry, J.-P.; Mazzei, G. J.; R. Bernard, A., Large scale transient expression with COS cells. *Cytotechnology* 1996, 18, 183-192.
58. Jordan, M.; Kohne, C.; Wurm, F. M., Calcium-phosphate mediated DNA transfer into HEK-293 cells in suspension: control of physicochemical parameters allows transfection in stirred media. Transfection and protein expression in mammalian cells *Cytotechnology* 1998, 26, 39-47.
59. Wurm, F.; Bernard, A., Large-scale transient expression in mammalian cells for recombinant protein production. *Curr Opin Biotechnol* 1999, 10, (2), 156-9.
60. Lindell, J.; Girard, P.; Muller, N.; Jordan, M.; Wurm, F., Calfection: a novel gene transfer method for suspension cells. *Biochim Biophys Acta* 2004, 1676, (2), 155-61.
61. Pham, P. L.; Perret, S.; Doan, H. C.; Cass, B.; St-Laurent, G.; Kamen, A.; Durocher, Y., Large-scale transient transfection of serum-free suspension-growing HEK293 EBNA1 cells: peptone additives improve cell growth and transfection efficiency. *Biotechnol Bioeng* 2003, 84, (3), 332-42.
62. Schlaeger, E. J.; Christensen, K., Transient gene expression in mammalian cells grown in serum-free suspension culture. *Cytotechnology* 1999, 30, (1-3), 71-83.
63. Schlaeger, E. J.; Kitas, E. A.; Dorn, A., SEAP expression in transiently transfected mammalian cells grown in serum-free suspension culture. *Cytotechnology* 2003, 42, (1), 47-55.
64. Girard, P.; Derouazi, M.; Baumgartner, G.; Bourgeois, M.; Jordan, M.; Jacko, B.; Wurm, F. M., 100-liter transient transfection. *Cytotechnology* 2002, 38, (1-3), 15-21.
65. Chu, L.; Robinson, D. K., Industrial choices for protein production by large-scale cell culture. *Curr Opin Biotechnol* 2001, 12, (2), 180-7.

66. Kelley, B. D., Biochemical engineering: Bioprocessing of therapeutic proteins. *Curr Opin Biotechnol* 2001, 12, (2), 173-4.
67. Cho, M. S.; Yee, H.; Brown, C.; Mei, B.; Mirenda, C.; Chan, S., Versatile expression system for rapid and stable production of recombinant proteins. *Biotechnol Prog* 2003, 19, (1), 229-32.
68. Graham, F. L.; Smiley, J.; Russell, W. C.; Nairn, R., Characteristics of a human cell line transformed by DNA from human adenovirus type 5. *J Gen Virol* 1977, 36, (1), 59-74.
69. Shen, E. S.; Cooke, G. M.; Horlick, R. A., Improved expression cloning using reporter genes and Epstein-Barr virus ori-containing vectors. *Gene* 1995, 156, (2), 235-9.
70. Graham, F. L., Growth of 293 cells in suspension culture. *J Gen Virol* 1987, 68 (Pt 3), 937-40.
71. Garnier, A.; Cote, J.; Nadeau, I.; Kamen, A.; Massie, B., Scale-up of the adenovirus expression system for the production of recombinant protein in human 293S cells. *Cytotechnology* 1994, 15, (1-3), 145-55.
72. Van Craenenbroeck, K.; Vanhoenacker, P.; Haegeman, G., Episomal vectors for gene expression in mammalian cells. *Eur J Biochem* 2000, 267, (18), 5665-78.
73. Foecking, M. K.; Hofstetter, H., Powerful and versatile enhancer-promoter unit for mammalian expression vectors. *Gene* 1986, 45, (1), 101-5.
74. Gorman, C. M.; Gies, D.; McCray, G.; Huang, M., The human cytomegalovirus major immediate early promoter can be trans-activated by adenovirus early proteins. *Virology* 1989, 171, (2), 377-85.
75. Massie, B.; Couture, F.; Lamoureux, L.; Mosser, D. D.; Guilbault, C.; Jolicoeur, P.; Belanger, F.; Langelier, Y., Inducible overexpression of a toxic protein by an adenovirus vector with a tetracycline-regulatable expression cassette. *J Virol* 1998, 72, (3), 2289-96.
76. Massie, B.; Mosser, D. D.; Koutroumanis, M.; Vitte-Mony, I.; Lamoureux, L.; Couture, F.; Paquet, L.; Guilbault, C.; Dionne, J.; Chahla, D.; Jolicoeur, P.; Langelier, Y., New adenovirus vectors for protein production and gene transfer. *Cytotechnology* 1998, 28, (1-3), 53-64.
77. Yates, J. L.; Warren, N.; Sugden, B., Stable replication of plasmids derived from Epstein-Barr virus in various mammalian cells. *Nature* 1985, 313, (6005), 812-5.
78. Belt, P. B.; Jongmans, W.; de Wit, J.; Hoeijmakers, J. H.; van de Putte, P.; Backendorf, C., Efficient cDNA cloning by direct phenotypic correction of a mutant human cell line (HPRT-) using an Epstein-Barr virus-derived cDNA expression vector. *Nucleic Acids Res* 1991, 19, (18), 4861-6.
79. Mazda, O.; Satoh, E.; Yasutomi, K.; Imanishi, J., Extremely efficient gene transfection into lympho-hematopoietic cell lines by Epstein-Barr virus-based vectors. *J Immunol Methods* 1997, 204, (2), 143-51.
80. Margolskee, R. F.; Kavathas, P.; Berg, P., Epstein-Barr virus shuttle vector for stable episomal replication of cDNA expression libraries in human cells. *Mol Cell Biol* 1988, 8, (7), 2837-47.
81. Carstens, C. P.; Gallo, J. C.; Maher, V. M.; McCormick, J. J.; Fahl, W. E., A system utilizing Epstein-Barr virus-based expression vectors for the functional cloning of human fibroblast growth regulators. *Gene* 1995, 164, (2), 195-202.
82. Seed, B., Developments in expression cloning. *Curr Opin Biotechnol* 1995, 6, (5), 567-73.
83. DuBridge, R. B.; Tang, P.; Hsia, H. C.; Leong, P. M.; Miller, J. H.; Calos, M. P., Analysis of mutation in human cells by using an Epstein-Barr virus shuttle system. *Mol Cell Biol* 1987, 7, (1), 379-87.
84. Kraus, E.; Strong, L. C.; Tainsky, M. A., pZ402, an improved SV40-based shuttle vector containing a T-antigen mutant unable to interact with wild-type p53. *Gene* 1998, 211, (2), 229-34.
85. Derouazi, M.; Girard, P.; Van Tilborgh, F.; Iglesias, K.; Muller, N.; Bertschinger, M.; Wurm, F. M., Serum-free large-scale transient transfection of CHO cells. *Biotechnol Bioeng* 2004, 87, (4), 537-45.

86. Reiter, M.; Hohenwarter, O.; Gaida, T.; Zach, N.; Schmatz, C.; Bluml, G.; Weigang, F.; Nilsson, K.; Katinger, H., The use of macroporous gelatin carriers for the cultivation of mammalian cells in fluidised bed reactors. *Cytotechnology* 1990, 3, (3), 271-7.
87. Nikolai, T. J.; Hu, W. S., Cultivation of mammalian cells on macroporous microcarriers. *Enzyme Microb Technol* 1992, 14, (3), 203-8.
88. Ulloa-Montoya, F.; Verfaillie, C. M.; Hu, W. S., Culture systems for pluripotent stem cells. *J Biosci Bioeng* 2005, 100, (1), 12-27.
89. Chevalot, I.; Visvikis, A.; Nabet, P.; Engasser, J. M.; Marc, A., Production of a membrane-bound protein, the human gamma-glutamyl transferase, by CHO cells cultivated on microcarriers, in aggregates and in suspension. *Cytotechnology* 1994, 16, (2), 121-9.
90. Tolbert, W. R.; Hitt, M. M.; Feder, J., Cell aggregate suspension culture for large-scale production of biomolecules. *In Vitro* 1980, 16, (6), 486-90.
91. Yamamoto, S.; Matsuda, H.; Takahashi, T.; Xing, X. H.; Tanji, Y.; Unno, H., Aggregate formation of rCHO cells and its maintenance in repeated batch culture in the absence of cell adhesion materials. *J Biosci Bioeng* 2000, 89, (6), 534-8.
92. Voisard, D.; Meuwly, F.; Ruffieux, P. A.; Baer, G.; Kadouri, A., Potential of cell retention techniques for large-scale high-density perfusion culture of suspended mammalian cells. *Biotechnol Bioeng* 2003, 82, (7), 751-65.
93. Liu, X. M.; Liu, H.; Wu, B. C.; Li, S. C.; Ye, L. L.; Wang, Q. W.; Huang, P. T.; Chen, Z. L., Suspended aggregates as an immobilization mode for high-density perfusion culture of HEK 293 cells in a stirred tank bioreactor. *Appl Microbiol Biotechnol* 2006, 72, (6), 1144-51.
94. Kretzmer, G., Industrial processes with animal cells. *Appl Microbiol Biotechnol* 2002, 59, (2-3), 135-42.
95. Kadouri, A.; Spier, R. E., Some myths and messages concerning the batch and continuous culture of animal cells. *Cytotechnology* 1997, 24, 89-98.
96. Portner, R.; Nagel-Heyer, S.; Goepfert, C.; Adamietz, P.; Meenen, N. M., Bioreactor design for tissue engineering. *J Biosci Bioeng* 2005, 100, (3), 235-45.
97. Al-Rubeai, M.; Singh, R. P.; Goldman, M. H.; Emery, A. N., Death mechanisms of animal cells in conditions of intensive agitation. *Biotechnol Bioeng* 1995, 45, (6), 463-72.
98. Kunas, K. T.; Papoutsakis, E. T., The protective effect of serum against hydrodynamic damage of hybridoma cells in agitated and surface-aerated bioreactors. *J Biotechnol* 1990, 15, (1-2), 57-69.
99. Gearing, D. P.; Gough, N. M.; King, J. A.; Hilton, D. J.; Nicola, N. A.; Simpson, R. J.; Nice, E. C.; Kelso, A.; Metcalf, D., Molecular cloning and expression of cDNA encoding a murine myeloid leukaemia inhibitory factor (LIF). *Embo J* 1987, 6, (13), 3995-4002.
100. Gough, N. M., Molecular genetics of leukemia inhibitory factor (LIF) and its receptor. *Growth Factors* 1992, 7, (3), 175-9.
101. Gearing, D. P., The leukemia inhibitory factor and its receptor. *Adv Immunol* 1993, 53, 31-58.
102. Moreau, J. F.; Donaldson, D. D.; Bennett, F.; Witek-Giannotti, J.; Clark, S. C.; Wong, G. G., Leukaemia inhibitory factor is identical to the myeloid growth factor human interleukin for DA cells. *Nature* 1988, 336, (6200), 690-2.
103. Baumann, H.; Wong, G. G., Hepatocyte-stimulating factor III shares structural and functional identity with leukemia-inhibitory factor. *J Immunol* 1989, 143, (4), 1163-7.
104. Hilton, D. J., LIF: lots of interesting functions. *Trends Biochem Sci* 1992, 17, (2), 72-6.
105. Samal, B. B.; Arakawa, T.; Boone, T. C.; Jones, T.; Prestrelski, S. J.; Narhi, L. O.; Wen, J.; Stearns, G. W.; Crandall, C. A.; Pope, J.; et al., High level expression of human leukemia inhibitory factor (LIF) from a synthetic gene in Escherichia coli and the physical and biological characterization of the protein. *Biochim Biophys Acta* 1995, 1260, (1), 27-34.
106. Escary, J. L.; Perreau, J.; Dumenil, D.; Ezine, S.; Brulet, P., Leukaemia inhibitory factor is necessary for maintenance of haematopoietic stem cells and thymocyte stimulation. *Nature* 1993, 363, (6427), 361-4.
107. Hilton, D. J.; Nicola, N. A.; Waring, P. M.; Metcalf, D., Clearance and fate of leukemia-inhibitory factor (LIF) after injection into mice. *J Cell Physiol* 1991, 148, (3), 430-9.

108. Metcalf, D., Polyfunctional cytokines: IL-6 and LIF. Introduction. *Ciba Found Symp* 1992, 167, 1-4.
109. Gearing, D. P.; Comeau, M. R.; Friend, D. J.; Gimpel, S. D.; Thut, C. J.; McGourty, J.; Brasher, K. K.; King, J. A.; Gillis, S.; Mosley, B.; et al., The IL-6 signal transducer, gp130: an oncostatin M receptor and affinity converter for the LIF receptor. *Science* 1992, 255, (5050), 1434-7.
110. Lord, K. A.; Abdollahi, A.; Thomas, S. M.; DeMarco, M.; Brugge, J. S.; Hoffman-Liebermann, B.; Liebermann, D. A., Leukemia inhibitory factor and interleukin-6 trigger the same immediate early response, including tyrosine phosphorylation, upon induction of myeloid leukemia differentiation. *Mol Cell Biol* 1991, 11, (9), 4371-9.
111. Okita, K.; Yamanaka, S., Intracellular signaling pathways regulating pluripotency of embryonic stem cells. *Curr Stem Cell Res Ther* 2006, 1, (1), 103-11.
112. Hilton, D. J.; Nicola, N. A.; Gough, N. M.; Metcalf, D., Resolution and purification of three distinct factors produced by Krebs ascites cells which have differentiation-inducing activity on murine myeloid leukemic cell lines. *J Biol Chem* 1988, 263, (19), 9238-43.
113. Williams, R. L.; Hilton, D. J.; Pease, S.; Willson, T. A.; Stewart, C. L.; Gearing, D. P.; Wagner, E. F.; Metcalf, D.; Nicola, N. A.; Gough, N. M., Myeloid leukaemia inhibitory factor maintains the developmental potential of embryonic stem cells. *Nature* 1988, 336, (6200), 684-7.
114. Hirayoshi, K.; Tsuru, A.; Yamashita, M.; Tomida, M.; Yamamoto-Yamaguchi, Y.; Yasukawa, K.; Hozumi, M.; Goeddel, D. V.; Nagata, K., Both D factor/LIF and IL-6 inhibit the differentiation of mouse teratocarcinoma F9 cells. *FEBS Lett* 1991, 282, (2), 401-4.
115. Pruitt, S. C.; Natoli, T. A., Inhibition of Differentiation by Leukemia Inhibitory Factor Distinguishes 2 Induction Pathways in P19 Embryonal Carcinoma-Cells. *Differentiation* 1992, 50, (1), 57-65.
116. Shen, M. M.; Leder, P., Leukemia inhibitory factor is expressed by the preimplantation uterus and selectively blocks primitive ectoderm formation in vitro. *Proc Natl Acad Sci U S A* 1992, 89, (17), 8240-4.
117. Stewart, C. L.; Kaspar, P.; Brunet, L. J.; Bhatt, H.; Gadi, I.; Kontgen, F.; Abbondanzo, S. J., Blastocyst implantation depends on maternal expression of leukaemia inhibitory factor. *Nature* 1992, 359, (6390), 76-9.
118. Melero-Martin, J. M.; Dowling, M. A.; Smith, M.; Al-Rubeai, M., Expansion of chondroprogenitor cells on macroporous microcarriers as an alternative to conventional monolayer systems. *Biomaterials* 2006, 27, (15), 2970-9.
119. Sambrook, J., *Molecular Cloning: A Laboratory Manual*. 3rd Edition ed.; Cold Spring Harbor Laboratory Press: 2001; p 999.
120. Lee, E. Y., Kinetic analysis of the effect of cell density on hybridoma cell growth in batch culture *Biotechnology and Bioprocess Engineering* 2002, 7, (2), 117-120.
121. Chioni, A. M.; Grose, R., Negative regulation of fibroblast growth factor 10 (FGF-10) by polyoma enhancer activator 3 (PEA3). *Eur J Cell Biol* 2009, 88, (7), 371-84.
122. Peshwa, M. V.; Kyung, Y. S.; McClure, D. B.; Hu, W. S., Cultivation of mammalian cells as aggregates in bioreactors: Effect of calcium concentration of spatial distribution of viability. *Biotechnol Bioeng* 1993, 41, (2), 179-87.
123. Moreira, J. L.; Alves, P. M.; Rodrigues, J. M.; Cruz, P. E.; Aunins, J. G.; Carrondo, M. J., Studies of baby hamster kidney natural cell aggregation in suspended batch cultures. *Ann N Y Acad Sci* 1994, 745, 122-33.
124. Goetghebeur, S.; Hu, W. S., Cultivation of anchorage-dependent animal cells in microsphere-induced aggregate culture. *Appl Microbiol Biotechnol* 1991, 34, (6), 735-41.
125. Nadeau, I.; Garnier, A.; Cote, J.; Massie, B.; Chavarie, C.; Kamen, A., Improvement of recombinant protein production with the human adenovirus/293S expression system using fed-batch strategies. *Biotechnol Bioeng* 1996, 51, (6), 613-23.
126. Newland, M.; Greenfield, P. F.; Reid, S., Hybridoma growth limitations: the roles of energy metabolism and ammonia production. *Cytotechnology* 1990, 3, (3), 215-29.

127. Sonnleitner, B.; Kappeli, O., Growth of Saccharomyces cerevisiae is controlled by its limited respiratory capacity: Formulation and verification of a hypothesis. *Biotechnol Bioeng* 1986, 28, (6), 927-37.
128. Borys, M. C.; Linzer, D. I.; Papoutsakis, E. T., Ammonia affects the glycosylation patterns of recombinant mouse placental lactogen-I by chinese hamster ovary cells in a pH-dependent manner. *Biotechnol Bioeng* 1994, 43, (6), 505-14.
129. Andersen, D. C.; Goochee, C. F., The effect of ammonia on the O-linked glycosylation of granulocyte colony-stimulating factor produced by chinese hamster ovary cells. *Biotechnol Bioeng* 1995, 47, (1), 96-105.
130. Weil, B. R.; Abarbanell, A. M.; Herrmann, J. L.; Wang, Y.; Meldrum, D. R., High glucose concentration in cell culture medium does not acutely affect human mesenchymal stem cell growth factor production or proliferation. *Am J Physiol Regul Integr Comp Physiol* 2009, 296, (6), R1735-43.
131. Biocarta Glycolysis Pathway. http://www.biocarta.com/pathfiles/h_glycolysis Pathway.asp (27 September),
132. Biocarta Catabolic Pathways for Arginine, Histidine, Glutamate, Glutamine, and Proline. http://www.biocarta.com/pathfiles/h_argininecPathway.asp (27 September),

6. Appendix

6.1. Carbon sources metabolism

Glucose preferred catabolism in mammalian cells is summarized in Figure 6.1, glycolysis. Pentose cycle can be an alternative from this route, starting from glucose-6-P to origin ribose-6-p and NADPH. In glycolysis, the six-carbon sugar glucose is oxidized and split in two halves, to create two molecules of pyruvate (3 carbons each) from each molecule of glucose. Along the way, the cell extracts a relatively small amount of energy from glucose in the form of ATP, 2 ATP molecules collected for each glucose molecule that starts down the glycolytic path. The pyruvate produced has one of three metabolic fates, to either become acetyl-CoA, ethanol, or lactate. When oxygen is available, the pyruvate can be converted to acetyl-CoA and enter the Krebs Cycle, where the acetyl-CoA will be completely oxidized and generate ATP through oxidative phosphorylation. Fermentation is much less efficient than oxidative phosphorylation in making ATP, creating only 2 ATP per glucose while oxidative phosphorylation creates 36 ATP per glucose in mammalian cells. Oxidative phosphorylation does not work in the absence of oxygen, however, and in the absence of oxygen glycolysis is forced to a halt due to a lack of NAD+, unless NAD+ is regenerated through fermentation.

Glutamine acts complementary as carbon source; the catabolism of glutamine is schematically represented in Figure 6.2. Glutamine is converted to glutamate by glutaminase or several other enzymes by the removal of the amide nitrogen. Transamination or deamination of glutamate produces a-ketoglutarate which feeds into the citric acid cycle.

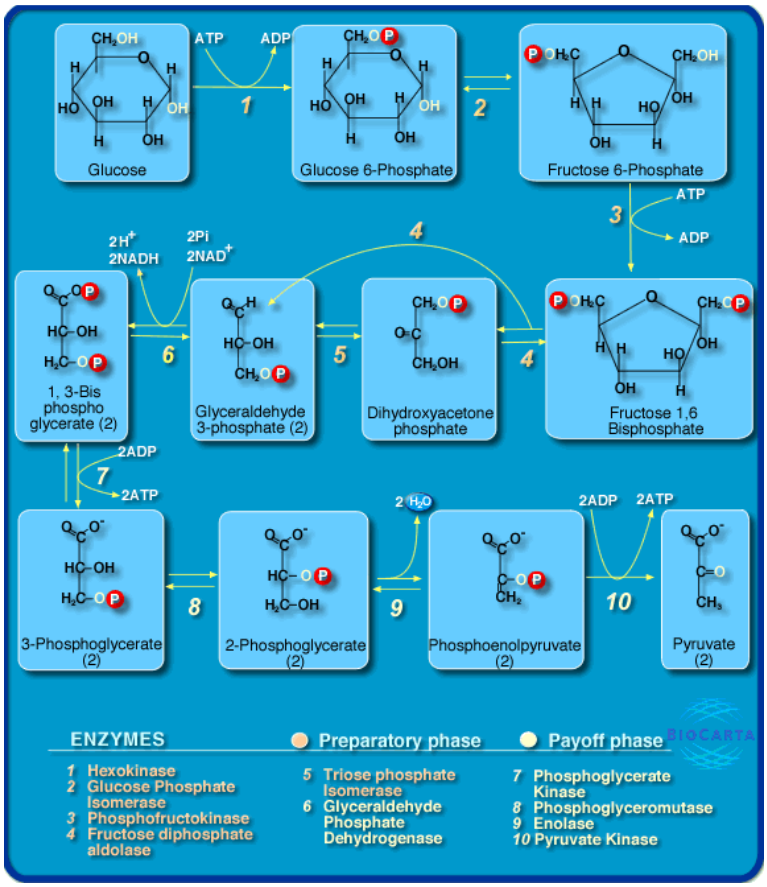

Figure 6.1 - Glycolysis Pathway in *Homo sapien.* Adapted from Biocarta [131]

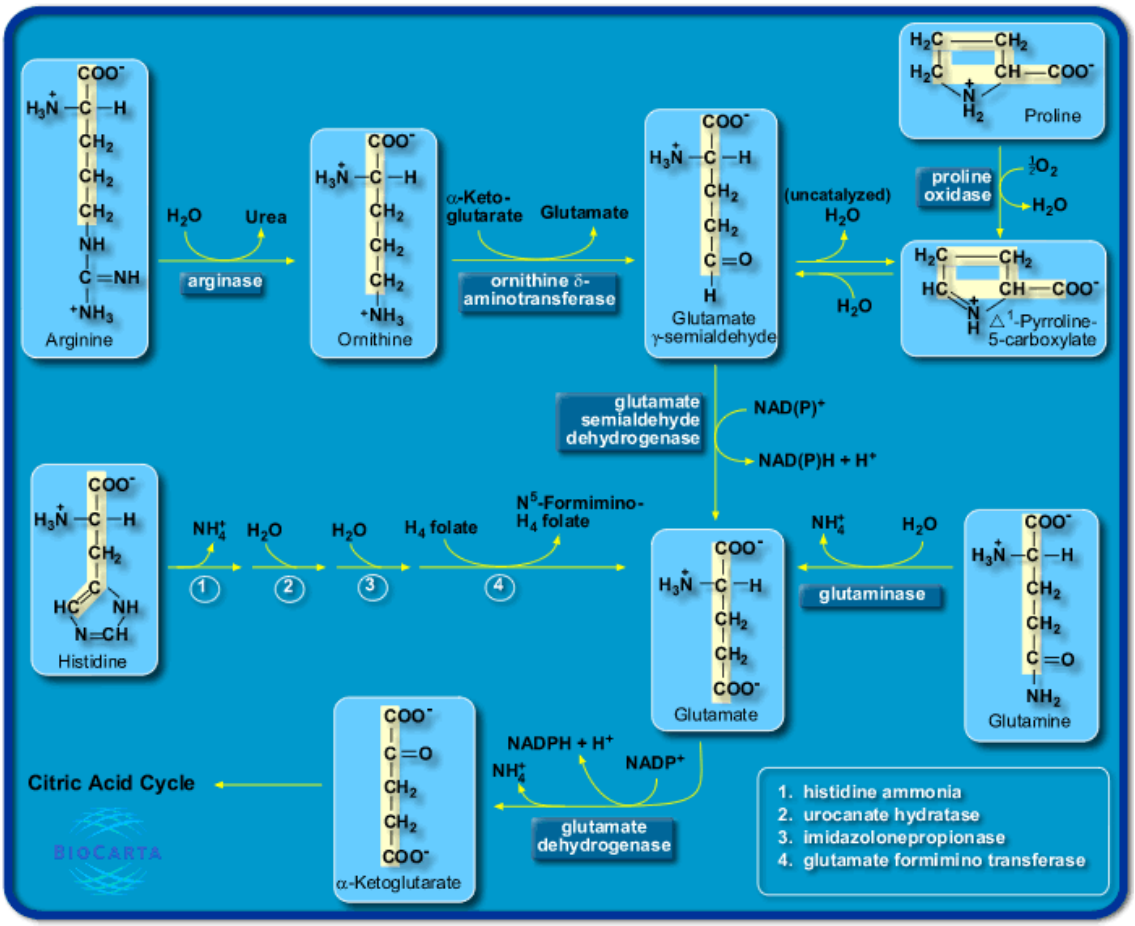

Figure 6.2 - Catabolic Pathways Glutamine, and Proline. Adapted from Biocarta [132]

6.2. Cell viability

Cell viability was controlled daily manually trough trypan blue exclusion method. Cell viability results are presented in Table 6.1. As observed in this data, HEK293-EBNA1 preserve high viability across all culture conditions, sustaining to be a preferred cell line for animal cell technology. In most of experiments cell viability was above 97%, except for the initial cell density of 2×10^6 cells.mL^{-1} and FR of 75% where, as discussed before, some operational error could have occurred. Negative values were not considered for average cell viability calculation.

Table 6.1 – Cell viability for each day of HEK293 culture (trypan blue exclusion method)

Initial cell density	2×10^4 cells.mL^{-1}	2×10^5 cells.mL^{-1}			2×10^6 cells.mL^{-1}		
FR / Day	**25%**	**25%**	**50%**	**75%**	**25%**	**50%**	**75%**
0	100%	100%	100%	94%	100%	100%	100%
1	93%	98%	96%	98%	100%	100%	100%
2	92%	99%	98%	96%	98%	100%	99%
3	98%	100%	100%	100%	100%	99%	98%
4	96%	100%	100%	98%	99%	98%	96%
5	100%	99%	100%	98%	99%	100%	91%
6	100%	100%	99%	100%	100%	98%	88%
7	100%	100%	100%	99%	100%	99%	83%
8	98%	-	-	98%	100%	98%	85%
9	95%	91%	97%	99%	100%	99%	79%
10	100%	100%	100%	94%	100%	99%	69%
11	94%	100%	99%	96%	100%	98%	72%
12	92%	100%	99%	99%	100%	99%	-178%
13	99%	99%	99%	100%			-76%
14	100%	100%	100%	99%			
15	98%	100%	100%	99%			
16	98%	100%	99%	99%			
17	90%	100%	100%	100%			
18	98%			99%			
19				-5%			
20							
Average Cell Viability	**97%**	**99%**	**99%**	**98%**	**100%**	**99%**	**88%**

Cell viability was tested also with LDH kit CytoTox96 (Promega) and compared with the previous data for the initial cell density of 2×10^6 cells.mL^{-1} and FR of 25%, obtained by trypan blue exclusion method. In Figure 6.3, the trypan blue methodology proves to be more accurate than spectrophotometric CytoTox96. CytoTox96 presents negative values for total cell number revealing that for lower rates of cell death the results are under the limit of detection of the method.

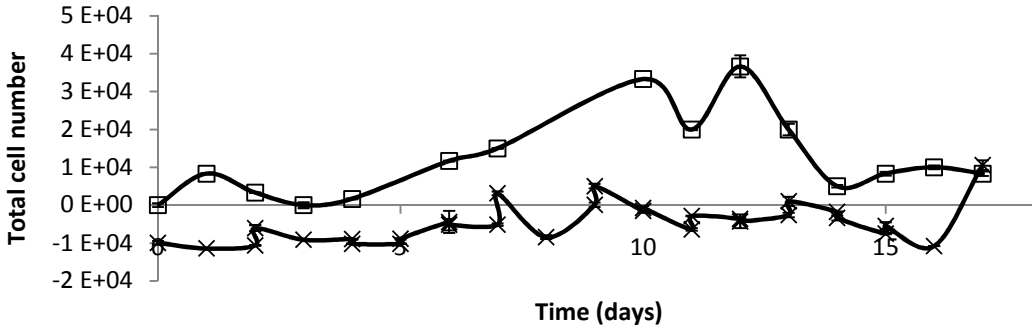

Figure 6.3 – Assessment of dead cell number by trypan blue exclusion method (⊟) and LDH kit CytoTox96 (✂) (Promega™). HEK293-EBNA1 cells at an initial cell density of 2×10^6 cells.mL^{-1} and FR of 25%,

Although the variability and accuracy of each method, when compared to the total cell number of viable cells, both methods support a low number of dead cells observed during culture time (lines are overhead), as is described in Figure 6.4.

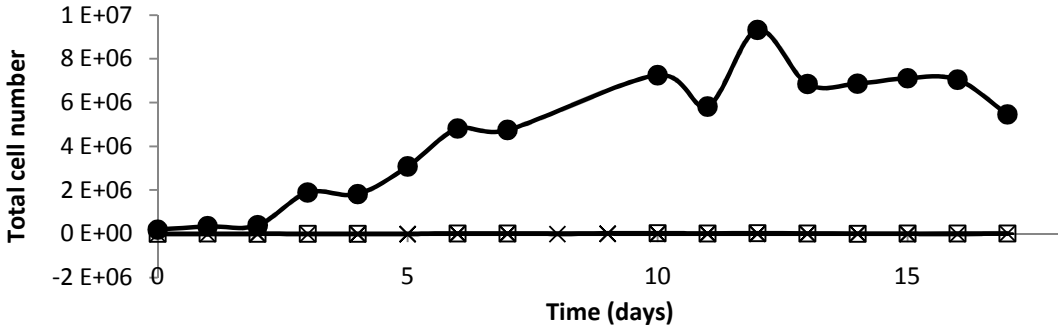

Figure 6.4 – Total cell number of HEK293 viable cells (●) compared to dead cells number by trypan blue exclusion method (⊟) and LDH kit CytoTox96 (✂) (Promega™). Initial cell density of 2×10^6 cells.mL^{-1} and FR of 25%.

6.3. Fitting curves to growth experimental data

Due to the great variability of experimental data it is difficult to establish an accurate exponential phase, being representative of overall culture growth. To help with this issue, a non-linear fitting was performed to all growth experiments using Origin® software using the Non Linear Curve Fit routine according to Equation 6.3:

$$Y = \frac{A_i - A_{i+1}}{1+(x/x_0)^p} + A_{i+1} \quad (6.3)$$

where A_i and A_{i+1} represent the viable cell number at day i and at day $i+1$, at corresponding times x_0 and x, respectively.

The software fits to experimental data (outlier points were previously excluded) and returns 100 points, statistical validated by ANOVA test. These output points were ploted in Microsoft Excel and a linear regression was established for exponential phase data, as can be seen in the model presented in Figure 6.5. From the linear regression equation $y = m.x + b$ can be obtained the μ_{max} (m value).

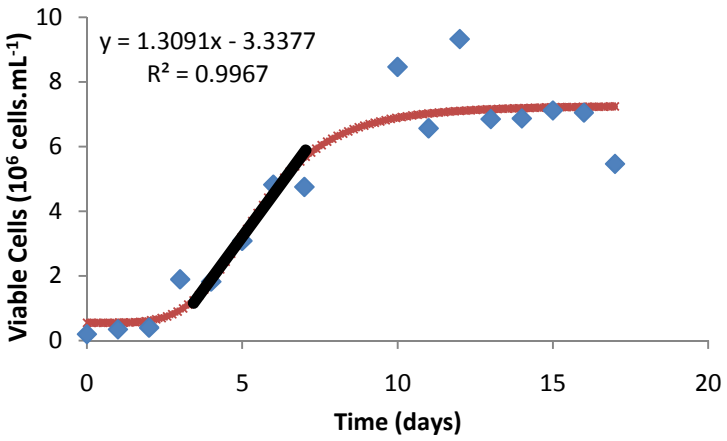

Figure 6.5 – Example of Non Linear Curve Fit to experimental data. The data reports the effect of feeding regime on growth of HEK293-EBNA1 in spinner flask and at 80 rpm Here is presented the initial cell density of 2×10^5 cells.mL^{-1} and a feeding regimen of 25% daily medium change. In red are presented the 100 points output Logistic regression for the experiment. In blue are presented the selected experimental data in the input of this function. The black line represents the linear regression to the points in the exponential part of growth, R^2 validates the accuracy of the linear regression.

6.4. Effect of feeding regime on growth, for an initial cell density of 2×10^6 cells.mL^{-1}

For the feeding regime tested in the present work (25%, 50% and 75% daily medium change), a higher initial cell density (2×10^6 cells.mL^{-1}) was also studied in order to better understand if it could be advantageous in terms of cell growth and recombinant protein productivity. The cell growth for this fed-batch experiment is shown in Figure 6.6.

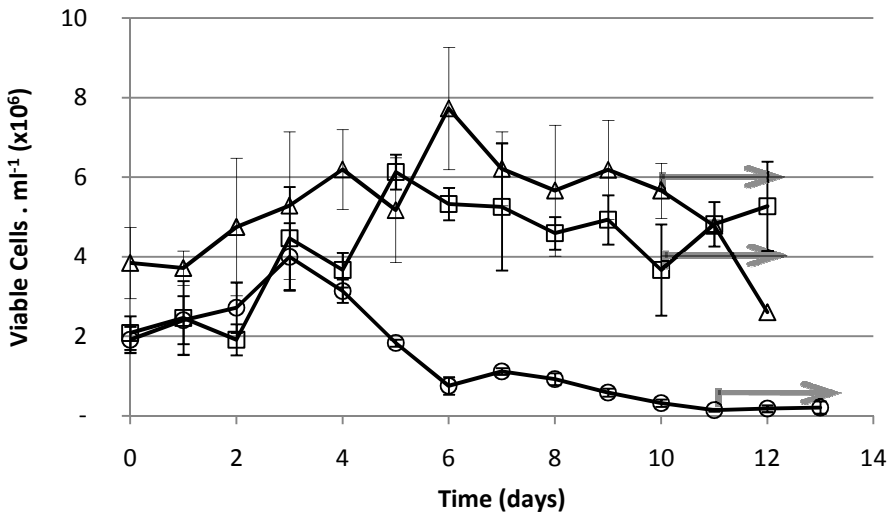

Figure 6.6 – Effect of feeding regime on growth of HEK293-EBNA1. Three feeding regime were tested: 25% (—▲—); 50% (—■—); 75% (—●—) of daily medium changes. Gray arrows indicate the production of human LIF in Serum-Free conditions.

Like in the previous set of experiments, also for the initial cell density of 2×10^6 cells.mL^{-1}, a higher cell expansion occurred in the 25% feeding regime. The 75% feeding regime incurred in cell loss after the third day. The motifs could be the ones mentioned before, as the high dilution of the autocrine signalling factors, responsible for proliferation regulation, but at this inoculum a more experimental factor can be addressed: a high inoculum lead to small aggregates and a great amount of cells in suspension as single cells) that resulted in loss of viable biomass with the medium removal, difficult to control, even with long time of cell sedimentation and cell recycle.

In the 25% and 50% feeding regime, the exponential phase was quite short and the stationary phase of growth occurred earlier, probably due to the high cell density

within the spinner flask volume. This strategy made possible to shorten the growth/production cycle in about 5 days when compared to the previous experiments, what could stand as an advantage. One of the major negative points in this high initial cell density (2×10^6 cells.ml^{-1}) strategy is related with the time and material consumption in inoculum production, the added value to culture maintenance and development of a large storage bank at low temperatures. Such disadvantage would be minimized if recycle of the cells after the fed-batch cycle could be successfully established. No analysis about the carbon source consumption (glucose and glutamine) and secondary metabolites production (lactate and ammonia) were performed for these experiments.

In Table 6.2, the specific growth rate was found to be quite similar both in 25% and 50% FR and therefore similar time of duplication. Higher cell expansion could be reached in 25% FR, apparently not significant in terms of the final cell density, similar with 50% FR.

Table 6.2 – Maximal growth rates, duplication time and maximal fold increase in total cell number for a inoculum of 2×10^5 cells.mL^{-1} at different feeding regimen in a spinner flask at 80 rpm.

Feeding Regime	μ_{max} (h^{-1})	t_d (h)	Fold Increase	X max (10^6 cells.mL^{-1})	X prod (10^6 cells.mL^{-1})
25 %	0.021	33.0	2.66	7.73	4.35
50 %	0.022	31.5	2.63	6.13	4.59
75 %	-	-	-	4.00	0.178

The higher medium renewal (75%) affected negatively the cell growth, corresponding to larger exponential phases and, consequently, lower μ_{max} values. Both 25% and 50% FR led to similar maximum fold increase, and also maximum growth rates were quite similar, 0.021 and 0.022, respectively. At these high initial cell densities, the growth phase is shorter being the steady phase plateau reached faster, achieving shorter culture times by production cycle – culture ends at day 12. Nevertheless, the 25% daily medium change confirmed to be the most useful and the most economic feeding regime strategy found to obtain the highest cell density. The 75% feeding regime registered negative value for μ_{max} (not presented) due to high cell loss.

The study of the effect of feeding regime, within the initial cell density of 2×10^6 cells.mL^{-1}, on the dynamic of cell aggregates is represented in Figure 6.7.

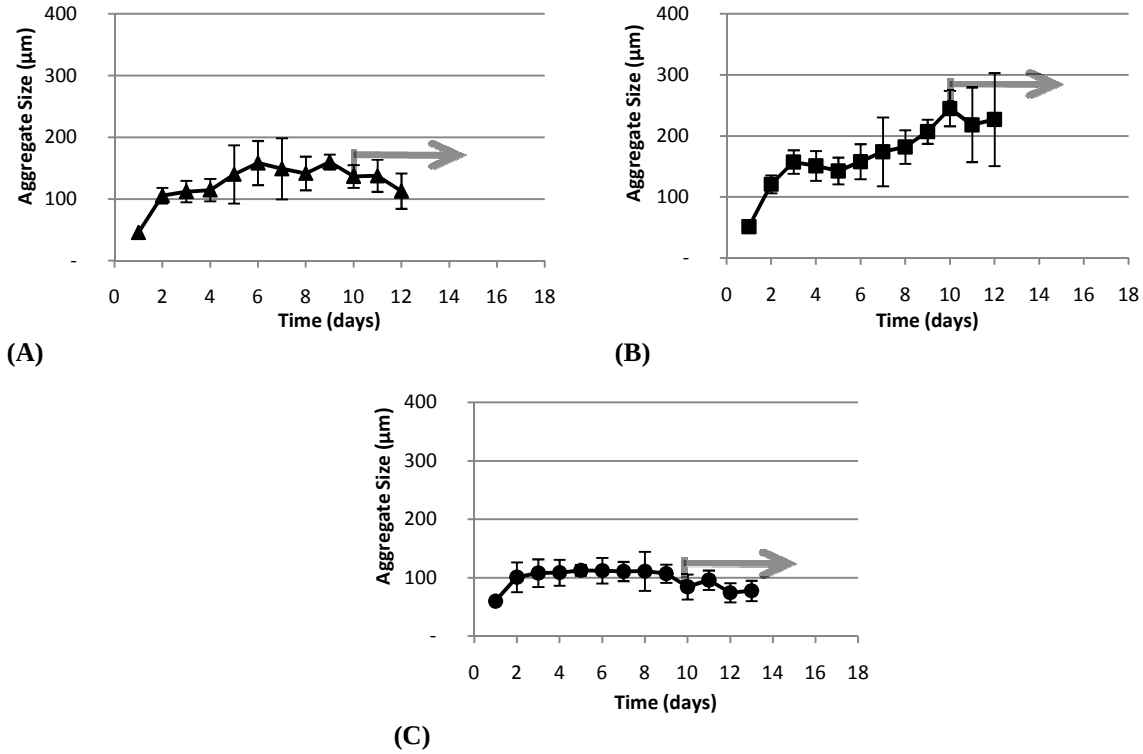

Figure 6.7 – Effect of initial cell density on aggregate size distribution of HEK293-EBNA1 in suspension culture. Three daily medium changes volumes were tested: 25% (—▲—); 75% (—■—); 75% (—●—) within an inoculum of 2×10^6 cells.mL^{-1} and an agitation rate of 80 rpm Gray arrows indicate the production of human LIF in Serum-Free conditions.

The average size of the cell aggregates increased with culture time, shifting from 46 µm, after 1 day, to approximately 160 µm, at day 6, for feeding regime of 25% (Figure 6.7A). For the feeding regime of 50% (Figure 6.7B), the aggregate sizes started in 51 µm, after 1 day, to a maximum of 245 µm. Relatively smaller aggregates were obtained for feeding regime of 75% (Figure 6.7C), shifting from 60 µm, after 1 day, to about 113 µm maximum. No cell aggregates within these condition reached sizes susceptible to diffusion limitations. If in the past set of experiments with the inoculum of 2×10^5 cells.mL^{-1} the feeding regime of 25% and 50% had similar hydrodynamics in cellular aggregate development, here it seems that the more availability in nutrients acted positively in increasing aggregates size. The 75% feeding regime, even with a higher nutrient availability could not undergo into larger aggregates, eventually by two

reasons: 1) the limited initial cell number did not allowed aggregate expansion; 2) the high volume perturbation interfered in aggregate stability.

Figure 6.8 indicates clearly that at this inoculum density and for all FR it was observed a large number of cells in suspension at the end of the culture time. In all the cases, it was observed a good homogeneity in aggregate size distribution.

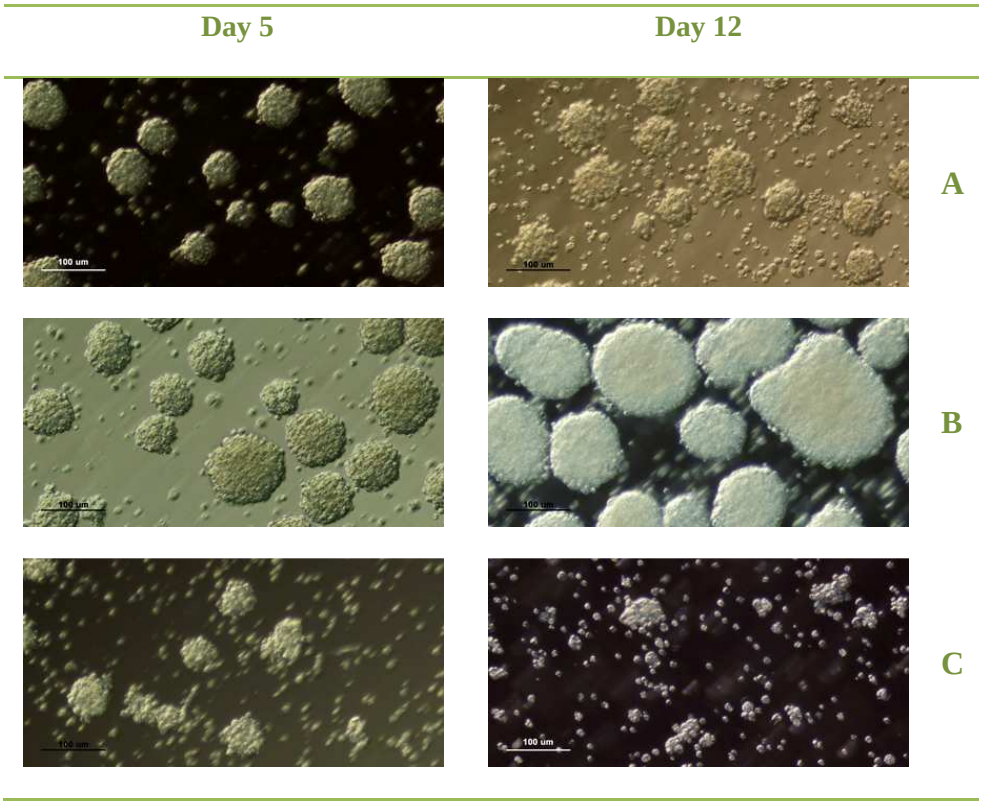

Figure 6.8 – Photograph of HEK293-EBNA1 cell aggregates along the culture (Day 5 and 12). A – feeding regimen of 25%; B – feeding regimen of 50%; C – feeding regimen of 75%, all with a start inoculum of 2×10^{6} cells.mL^{-1} and with daily medium change. Scale bar represents 100 μm.

In Figure 6.8C is evident the incapacity of growth and aggregate expansion of the culture. Here, microscopy photographs support the statistical data about aggregate hydrodynamics. This data suggests that higher volume perturbations on the system may be negative to cell growth and also for hydrodynamics consistency and morphology of aggregates, confirming the data obtained in the cultures with the initial cell density of 2×10^{5} cells.mL^{-1}. As previously discussed, the cell aggregate diameters for these experiments are still far from any hypothesis of nutrient diffusion limitations.